



# Distinct Notch1 and *BCL11B* requirements mediate human $\gamma\delta/\alpha\beta$ T cell development

Anne-Catherine Dolens<sup>1</sup>, Kaat Durinck<sup>2,†</sup>, Marieke Lavaert<sup>1,†</sup>, Joni Van der Meulen<sup>2,†</sup>, Imke Velghe<sup>1</sup>, Jelle De Medts<sup>1</sup>, Karin Weening<sup>1</sup>, Juliette Roels<sup>1,2</sup>, Katrien De Mulder<sup>1</sup>, Pieter-Jan Volders<sup>2</sup>, Katleen De Preter<sup>2</sup>, Tessa Kerre<sup>1</sup>, Bart Vandekerckhove<sup>1</sup>, Georges Leclercq<sup>1</sup>, Jo Vandesompele<sup>2</sup> , Pieter Mestdagh<sup>2</sup>, Pieter Van Vlierberghe<sup>2</sup> , Frank Speleman<sup>2</sup> & Tom Taghon<sup>1,\*</sup> 

## Abstract

$\gamma\delta$  and  $\alpha\beta$  T cells have unique roles in immunity and both originate in the thymus from T-lineage committed precursors through distinct but unclear mechanisms. Here, we show that Notch1 activation is more stringently required for human  $\gamma\delta$  development compared to  $\alpha\beta$ -lineage differentiation and performed paired mRNA and miRNA profiling across 11 discrete developmental stages of human T cell development in an effort to identify the potential Notch1 downstream mechanism. Our data suggest that the *miR-17-92* cluster is a Notch1 target in immature thymocytes and that miR-17 can restrict *BCL11B* expression in these Notch-dependent T cell precursors. We show that enforced miR-17 expression promotes human  $\gamma\delta$  T cell development and, consistently, that *BCL11B* is absolutely required for  $\alpha\beta$  but less for  $\gamma\delta$  T cell development. This study suggests that human  $\gamma\delta$  T cell development is mediated by a stage-specific Notch-driven negative feedback loop through which miR-17 temporally restricts *BCL11B* expression and provides functional insights into the developmental role of the disease-associated genes *BCL11B* and the *miR-17-92* cluster in a human context.

**Keywords** human; miRNA; Notch1; thymus;  $\gamma\delta$  T cell

**Subject Categories** Immunology; RNA Biology; Signal Transduction

**DOI** 10.15252/embr.201949006 | Received 5 August 2019 | Revised 3 March 2020 | Accepted 12 March 2020 | Published online 7 April 2020

**EMBO Reports (2020) 21: e49006**

## Introduction

T lymphocytes express either the  $\alpha\beta$  or the  $\gamma\delta$  T cell receptor (TCR), and both T cell lineages develop in the thymus from common precursors. During this tightly regulated process, developing thymocytes pass through discrete developmental stages and checkpoints to ensure that only functional, non-self-reactive T cells are released

into the periphery [1,2]. Activation of Notch signaling is a major driver of early T cell development. In mammals, the Notch pathway is comprised of 5 Notch ligands that belong to the Delta-like ligand (DLL-1, -3, -4) or Jagged (JAG1, -2) families and these can activate 4 Notch receptors (Notch 1-4). Within the thymus, DLL4 activates Notch1 on immigrating hematopoietic progenitor cells (HPCs) to induce T-lineage specification [3-5], and Notch1 activation in turn then induces expression of *BCL11B* that marks T-lineage commitment. Subsequently, the developing thymocytes rearrange their TCRs to become  $\alpha\beta$  or  $\gamma\delta$  T cells. In mice, Notch activation rises until the  $\beta$ -selection checkpoint and further maturation of  $\alpha\beta$ -lineage cells is more stringently dependent on Notch signaling compared to  $\gamma\delta$  development [6-8]. Following  $\beta$ -selection, Notch activation no longer seems required for thymocyte maturation [9] although some reports suggest a role in CD8 T cell development [10-13]. Different Notch signaling kinetics and requirements are observed during early T cell development in humans. The highest Notch activation level is reached at the T-lineage specification stage and it declines thereafter, earlier than in mouse [2,14], during T-lineage commitment in a GATA3-dependent manner [15]. In humans, lower Notch activity is also required for efficient TCR $\alpha\beta$ -lineage differentiation, whereas  $\gamma\delta$  T cell development is highly Notch-dependent [14] and partially involves JAG2/Notch3 interactions [16].

The precise molecular mechanism that controls Notch-driven  $\gamma\delta$  T cell development in humans has remained unclear and in general, little is known on the molecular drivers of human  $\gamma\delta$  T cell development despite the growing interest in using them for immunotherapy. Also in mouse models, only a limited number of molecular pathways have been identified that influence the developmental choice between  $\alpha\beta$ - and  $\gamma\delta$ -lineage cells. Besides TCR signal strength [17-19] and Notch signaling [6,7], few other specific transcriptional regulators have also been implicated [20-22]. One example is *BCL11B* which, following induction of T-lineage commitment [23,24], is also stringently required for  $\alpha\beta$  T cell development but not for  $\gamma\delta$ -lineage differentiation. While most knowledge is derived from murine experiments, some of these mechanisms differ in

1 Department of Diagnostic Sciences, Ghent University, Ghent, Belgium

2 Department of Biomolecular Medicine, Ghent University, Ghent, Belgium

\*Corresponding author. Tel: +32 9 332 01 33; Fax: +32 9 332 36 59; E-mail: tom.taghon@ugent.be

† These authors contributed equally to this work

humans [25]. Importantly, a clear understanding of the molecular drivers of human T cell development is however critical for understanding mechanisms of disease, such as in case of leukemia or immune deficiency.

Here, we profoundly investigated the role of Notch1, DLL4, and JAG2 in human  $\gamma\delta$  development and determined the mRNA and miRNA profiles of 11 stages of human T cell development, including developing  $\gamma\delta$  T cells, in an effort to reveal the molecular mechanisms that mediate Notch-driven  $\gamma\delta$ -lineage differentiation. Our results reveal that developing human  $\alpha\beta$  and  $\gamma\delta$  T cells have different Notch and BCL11B requirements and suggest that this involves miR-17 activity that functions as a Notch-driven negative feedback loop that limits BCL11B expression during early human T cell development, thereby promoting  $\gamma\delta$ -lineage differentiation. Moreover, our dataset provides novel molecular insights into the mRNA/miRNA network that controls human T cell development, including during the  $\alpha\beta$  versus  $\gamma\delta$  bifurcation, and thus is of clear translational relevance.

## Results

### Human $\gamma\delta$ T cell development is more Notch1/DLL4/JAG2-dependent compared to TCR $\alpha\beta$ T cell development

Inhibition of JAG2-mediated Notch3 activation results in a significant, but partial reduction in human TCR $\gamma\delta$  development [16]. To investigate the role of Notch1, we performed fetal thymus organ cultures (FTOCs) in which murine fetal days 14–15 thymic lobes were reconstituted with human CD34<sup>+</sup>CD1<sup>-</sup> uncommitted thymocytes in the presence of blocking Notch1 antibody (Fig 1A–C). In this setting, the murine thymic lobes serve as a physiological micro-environment that supports the differentiation of human progenitors into T cells [26,27]. Consistent with pan-Notch inhibition studies [14], Notch1 blocking resulted in significant higher frequencies of CD4<sup>+</sup>CD8 $\beta$ <sup>+</sup> double-positive (DP) and CD3<sup>+</sup>TCR $\alpha\beta$ <sup>+</sup> thymocytes but had little effect on the absolute number of these  $\alpha\beta$ -lineage cells. In contrast, TCR $\gamma\delta$  T cell development was significantly reduced, also in absolute numbers (Fig 1A–C). Since Notch1 can be activated by DLL4 and JAG2 on the thymic epithelial cells (TECs) [28], we initiated FTOCs with thymic lobes from *Dll4<sup>fl/fl</sup>Jag2<sup>fl/fl</sup>* mice that were crossed with FoxN1-Cre mice to induce TEC-specific gene deletion [16]. Compared to *Cre<sup>-</sup>* control lobes,  $\gamma\delta$  development significantly and dose-dependently decreased upon deletion of Notch ligand alleles in *Dll4<sup>wt/fl</sup>Jag2<sup>wt/fl</sup>*

*Cre<sup>+</sup>*, *Dll4<sup>wt/fl</sup>Jag2<sup>fl/fl</sup>Cre<sup>+</sup>*, *Dll4<sup>fl/fl</sup>Jag2<sup>wt/fl</sup>Cre<sup>+</sup>*, and *Dll4<sup>fl/fl</sup>Jag2<sup>fl/fl</sup>Cre<sup>+</sup>* FTOCs, respectively (Fig 1D–F). In contrast, the development of DP and CD3<sup>+</sup>TCR $\alpha\beta$ <sup>+</sup> thymocytes was not inhibited but rather enhanced, although not significantly, as long as one JAG2 or DLL4 allele was maintained (Fig 1D–F). Deletion of *Jag1* did not affect human T cell development (Appendix Fig S1A and B), confirming that DLL4 and JAG2 are the relevant ligands for early human T cell development [28]. Through OP9-DLL4 coculture experiments, we investigated whether rearranged TCR $\gamma\delta$  expressing thymocytes [29] still displayed this Notch dependency (Fig EV1). Interestingly, uncommitted TCR $\gamma\delta$ <sup>+</sup>CD3<sup>+</sup>CD28<sup>+</sup>CD1a<sup>+</sup>CD73<sup>-</sup> thymocytes still remained dependent on Notch activation (Fig EV1A, C and D), particularly the expansion of immature CD1a<sup>+</sup>TCR $\gamma\delta$  expressing thymocytes was clearly and repetitively reduced upon addition of a  $\gamma$ -secretase inhibitor (GSI) (Fig EV1E) although this did not reach significance in a paired *t*-test, most likely due to donor variability in cellular output from these cultures. In contrast, committed TCR $\gamma\delta$ <sup>+</sup>CD3<sup>+</sup>CD28<sup>+</sup>CD1a<sup>+</sup>CD73<sup>+</sup> thymocytes efficiently matured into CD1a<sup>-</sup>  $\gamma\delta$  T cells, a stage where Notch no longer is required for human  $\gamma\delta$  T cell development as also observed from a subset of the CD73<sup>-</sup> uncommitted TCR $\gamma\delta$ <sup>+</sup> thymocytes that matured in CD1a<sup>-</sup>  $\gamma\delta$  T cells (Fig EV1B and F). Overall, these results reveal that human  $\gamma\delta$  T cell development is highly dependent on Notch1 activation and that this, at least in part, relates to the proliferation of immature  $\gamma\delta$  T cells.

### mRNA profiling reveals major shifts in gene expression upon developmental divergence of human $\gamma\delta$ - and $\alpha\beta$ -lineage cells

To understand the mechanisms that drive human  $\gamma\delta$  development, we performed genome-wide mRNA expression analysis of 11 developmental stages of human T cell development (Fig EV2), including the  $\beta$ -selection checkpoint [30] and immature (CD1a<sup>+</sup>) and mature (CD1a<sup>-</sup>)  $\gamma\delta$  T cells, subsets that were previously omitted [31–33]. We also included cord blood (CB) CD34<sup>+</sup>Lin<sup>-</sup> cells as a reference subset of extrathymic HPCs to facilitate the identification of T-lineage genes. A strong correlation was observed between both independent donors (Appendix Fig S2) and gene expression analysis for markers used for sorting (*CD1A*, *CD34*, *CD4*) and of known important (*LMO2*, *GATA3*, *TCF7*) and stage-specific (*PTCRA*, *TRAC*, *RAG1*) genes during T cell development, including immature (*MYC*),  $\alpha\beta$ -lineage (*RORC*) [34], and  $\gamma\delta$ -lineage genes (*ZBTB16* encoding PLZF) [35] validated our approach (Fig 2A). Unsupervised hierarchical clustering yielded the expected developmental sequence of human T cell development, with immature CD34<sup>+</sup> subsets

#### Figure 1. Human TCR $\gamma\delta$ T cell development is more Notch1/DLL4/JAG2-dependent compared to TCR $\alpha\beta$ T cell development.

- A Flow cytometry analysis of CD34<sup>+</sup>CD1a<sup>-</sup> thymocytes cultured in FTOCs, in the presence of a control or anti-Notch1 blocking antibody. Numbers in dot plots indicate percentage of cells for the corresponding populations. Histograms show TCR $\gamma\delta$  expression in CD3<sup>+</sup>TCR $\alpha\beta$ <sup>+</sup> (blue) and CD3<sup>+</sup>TCR $\alpha\beta$ <sup>-</sup> (red) cells.
- B, C (B) Mean frequency and (C) absolute cell numbers of human CD4<sup>+</sup>CD8 $\beta$ <sup>+</sup> DP (black shades), CD3<sup>+</sup>TCR $\alpha\beta$ <sup>+</sup> (blue shades), and CD3<sup>+</sup>TCR $\gamma\delta$ <sup>+</sup> (red shades) thymocytes developed in corresponding cultures from (A) (*n* = 6 independent experiments with different donors; error bars indicate SEM, and \* indicates *P* < 0.05 and ns (not significant) indicates *P* > 0.05 in a non-parametric paired Wilcoxon test).
- D Flow cytometry analysis of CD34<sup>+</sup>CD1a<sup>-</sup> thymocytes submitted to FTOC with fetal thymic lobes deficient for *Dll4* and/or *Jag2* (*Cre<sup>+</sup>*) as indicated above the dot plots. Numbers in dot plots indicate percentage of cells for the corresponding populations. Histograms show TCR $\gamma\delta$  expression in CD3<sup>+</sup>TCR $\alpha\beta$ <sup>+</sup> (blue) and CD3<sup>+</sup>TCR $\alpha\beta$ <sup>-</sup> (red) cells.
- E, F (E) Mean frequency and (F) absolute cell numbers of CD3<sup>+</sup>TCR $\alpha\beta$ <sup>+</sup> (blue) and CD3<sup>+</sup>TCR $\gamma\delta$ <sup>+</sup> (red) thymocytes developed in corresponding cultures from (D) (*n* = 5–7 independent experiments, depending on the mouse genotype; error bars indicate SEM, and \* indicates *P* < 0.05 and ns (not significant) indicates *P* > 0.05 in a non-parametric Mann–Whitney *U*-test).

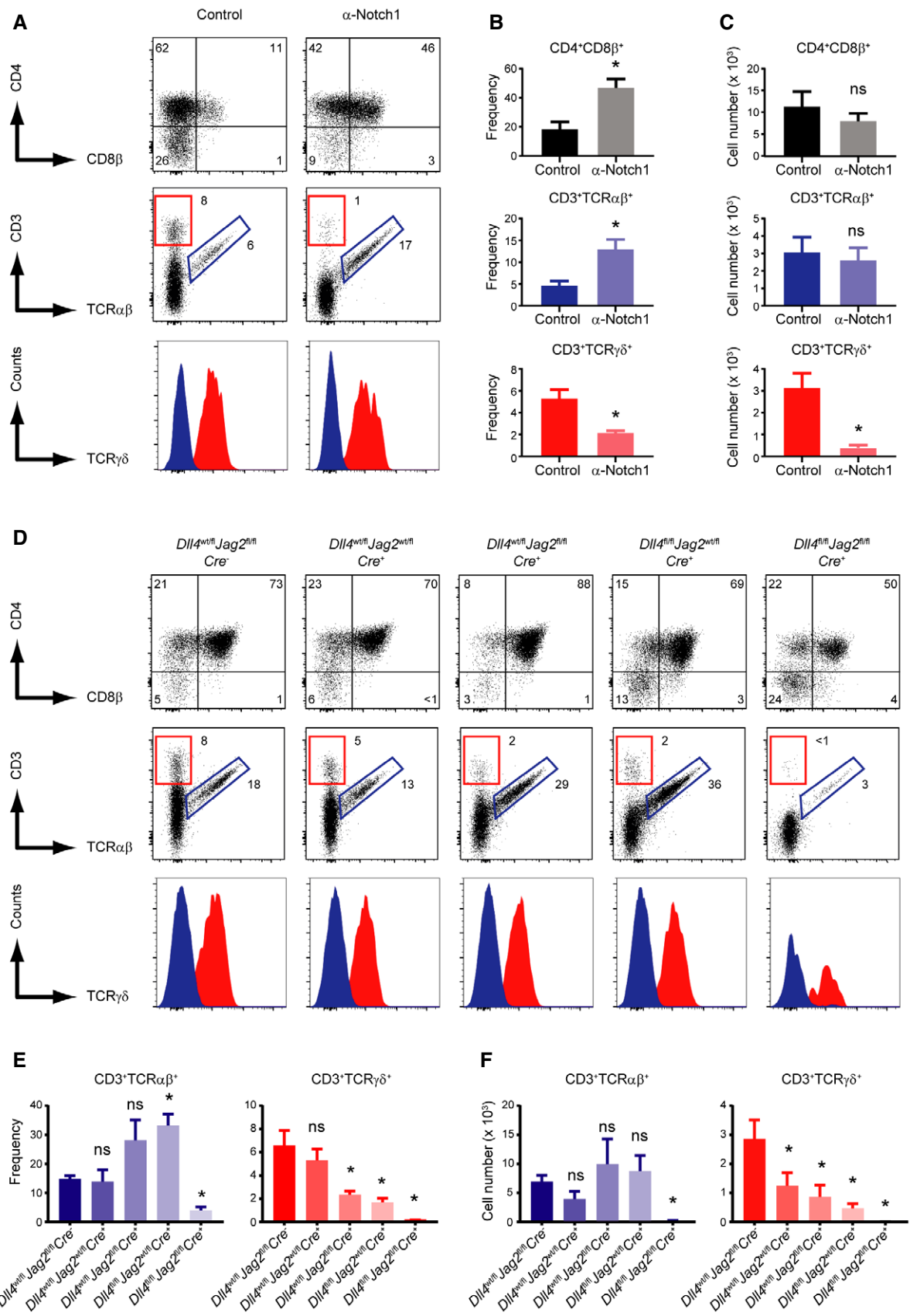


Figure 1.

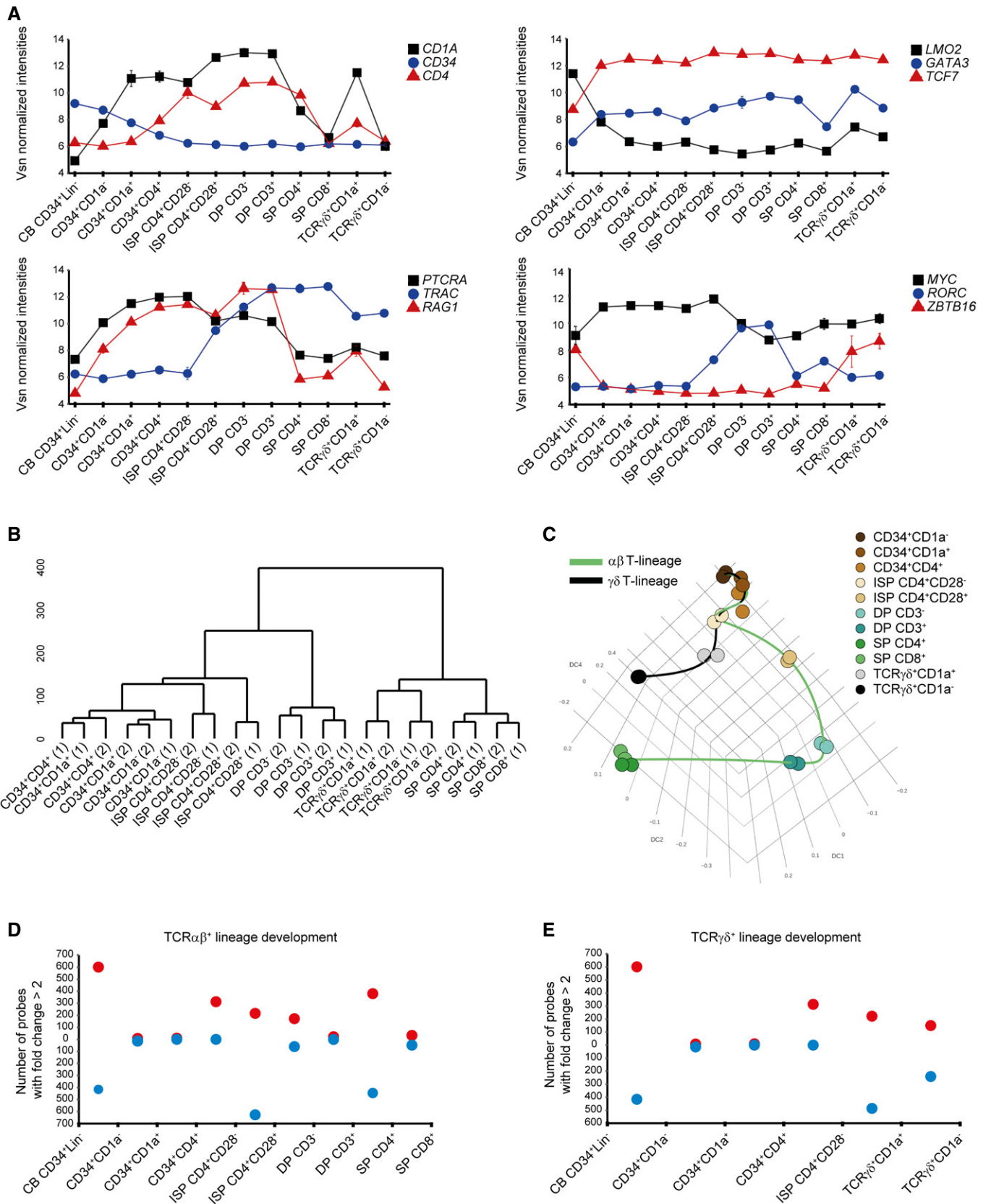


Figure 2.



**Figure 2. Global analysis of the transcriptome across distinct T cell subsets reflects development.**

- A Line plots depicting fluctuations in gene expression levels from vsn normalized probe intensities across human T cell development for both  $\alpha\beta$ - and  $\gamma\delta$ -lineages ( $n = 2$  biological replicates; error bars indicate SEM).
- B Dendrogram classifying the T cell developmental subsets and replicates, based on the normalized mRNA expression.
- C Diffusion map, displaying diffusion component (DC) 1, 2, and 4, generated from the mRNA expression profiles reconstructing the developmental trajectories of the  $\alpha\beta$  and  $\gamma\delta$  developmental lineages across human thymocyte subsets. The line connecting the different subsets is reflecting the developmental stages of human T cell development.
- D, E Scatterplot displaying the up (red)- or down (blue)regulation of probes ( $\log_2$  fold change  $\geq 2$ ) identified by sequential pairwise comparisons across either  $\alpha\beta$  (D) or  $\gamma\delta$  (E) development.

clustering together ( $CD34^+$  and immature single-positive  $CD4^+$  ( $ISP4^+$ ) subsets), as well as TCR expressing SP and immature and mature  $\gamma\delta$  T cell subsets (Fig 2B). Consistent with experiments that suggested that  $\gamma\delta$ - and  $\alpha\beta$ -lineages diverge after the pre- $\beta$ -selection  $ISP\ CD4^+CD28^-$  stage [30], diffusion map analysis illustrated the magnitude of differences and distinct developmental paths that immature  $TCR\gamma\delta^+CD1a^+$  and  $\alpha\beta$ -lineage DP cells follow when differentiating toward mature  $TCR\gamma\delta$  and  $CD4$  or  $CD8\ TCR\alpha\beta$  T cells (Fig 2C). Analysis of stage-specific gene expression changes during  $TCR\alpha\beta$  (Fig 2D) and  $TCR\gamma\delta$  (Fig 2E) development confirmed that, following T-lineage specification ( $CB\ CD34^+Lin^-$  vs thymocyte  $CD34^+CD1a^-$  comparison), the major transcriptional changes occurred at these  $\beta$ - and  $\gamma\delta$ -selection checkpoints, as well as at the DP to SP transition during  $TCR\alpha\beta$  T cell development. This involved both up- and downregulation of genes. Few changes occurred during T-lineage commitment ( $CD34^+CD1a^-$  to  $CD34^+CD1a^+$ ), while a set of genes was specifically upregulated at the  $CD34^+CD4^+$  to  $ISP\ CD4^+CD28^-$  transition. Similar as in mouse,  $CD4$  and  $CD8$  SP cells had very similar gene expression patterns [36]. Thus, diverging  $\alpha\beta$ - and  $\gamma\delta$ -lineage cells display distinct mRNA expression profiles.

**miRNA profiling uncovers novel regulatory changes during normal human T cell development**

To reveal a novel layer in the molecular regulation of human T cell development, we determined the expression of 756 miRNAs in the same thymocyte samples, with again good correlation between both samples (Appendix Fig S3). Unsupervised clustering, using the 216 miRNAs that showed expression in both replicates of at least 1 developmental stage, yielded the anticipated sequence of T cell development, with the exception of immature  $TCR\gamma\delta^+CD1a^+$  T cells that clustered more closely with the most immature stages, suggesting similar miRNA profiles (Fig 3A). Diffusion map analysis using these miRNAs was also sufficient to recapitulate the developmental divergence between both T cell lineages, suggesting that miRNAs mediate this process (Fig 3B). Consistent with the induction of specific genes during the  $CD34^+$  to  $ISP\ CD4^+CD28^-$  transition (Fig 2D), more miRNAs were downregulated then upregulated at this point (Fig 3C and D), suggesting a possible link. At  $\beta$ -selection, a specific group of miRNAs was downregulated, whereas the subsequent transition from  $ISP\ CD4^+CD28^+$  into DP thymocytes was mainly characterized by an increase in miRNA expression (Fig 3C). And while maturation from DP cells into SP thymocytes was characterized by both an up- and downregulation of miRNAs, few miRNAs differed between SP  $CD4$  and  $CD8$  T cells, consistent with their similar mRNA profiles. In contrast to  $\beta$ -selection,  $\gamma\delta$ -selection mainly involved upregulation of miRNAs, whereas further maturation into  $TCR\gamma\delta^+CD1a^-$  T cells was accompanied by

downregulation of miRNAs (Fig 3D). These data reveal dynamic regulation of miRNA expression during human T cell development with differences between developing  $\alpha\beta$ - and  $\gamma\delta$ -lineage cells.

**Notch1-correlated miRNAs during human T cell development**

Given that strong Notch activation favors human  $\gamma\delta$  T cell development, we sought to identify Notch-dependent miRNAs that support this process. *NOTCH1* expression is confined to the immature stages of T cell development and declines after  $\beta$ -selection (Fig 4A and B) [8,30], corresponding to stages of Notch activation as illustrated by the expression of its correlated targets *HES1* and *MYC* (Fig 4A and B). Correlation analysis revealed miRNAs with a similar expression pattern as *NOTCH1*, including all members of the miR-17–92 cluster (Fig 4B), suggesting Notch-dependent regulation. To functionally validate this, we determined the mRNA and miRNA expression profiles of  $CD34^+$  thymocytes in which Notch activity was modulated through coculture on OP9 cells that do or do not express a particular Notch ligand [28]. Canonical Notch targets (*MYC*, *NOTCH3*, *IL7R*, *HES1*) and *NOTCH1* itself were expressed in non-cultured *ex vivo* isolated thymocytes and in those that were exposed to OP9 cells expressing Notch ligands, but not upon OP9 control coculture (Fig 4C), validating our approach. From the *NOTCH1*-correlated miRNAs in culture (Fig 4D), some overlapped with the *NOTCH1*-correlated miRNAs during T cell development (Fig 4B). These include several members of the *miR-17–92* cluster that showed ICN1 and CSL binding in ChIP-seq experiments (Fig 4E) [37]. These findings are consistent with the possible direct regulation of the *miR-17–92* locus by Notch1.

**miR-17 targets BCL11B during thymocyte development**

To identify target genes for the Notch1-correlated miRNAs that could mediate Notch-driven  $\gamma\delta$  T cell development, we used two prediction databases and looked for potential targets within the genes that showed differential expression between  $\alpha\beta$ - and  $\gamma\delta$ -lineage cells (Appendix Fig S4). Interestingly, *BCL11B* was a predicted target for both miR-17 and miR-92a, consistent with the observation that *Bcl11b*-deficient mice exhibit a defect in  $TCR\alpha\beta$  T cell development, but not in  $TCR\gamma\delta$  differentiation [38]. The 3'UTR region of *BCL11B* contains 3 potential miR-17 and 1 potential miR-92a binding site (Fig 5A), and functional assessment using a 3'UTR luciferase assay in which pre-miR miRNA precursors were transfected revealed specific targeting by miR-17, and not by miR-92a, which was blocked upon mutation of those miR-17 binding sites (Fig 5B). Consistently, independent viral-mediated overexpression of *miR-17* in  $CD34^+$  thymocytes reduced *BCL11B* expression (Fig 5C). Furthermore, miR-17 knockdown, through overexpression

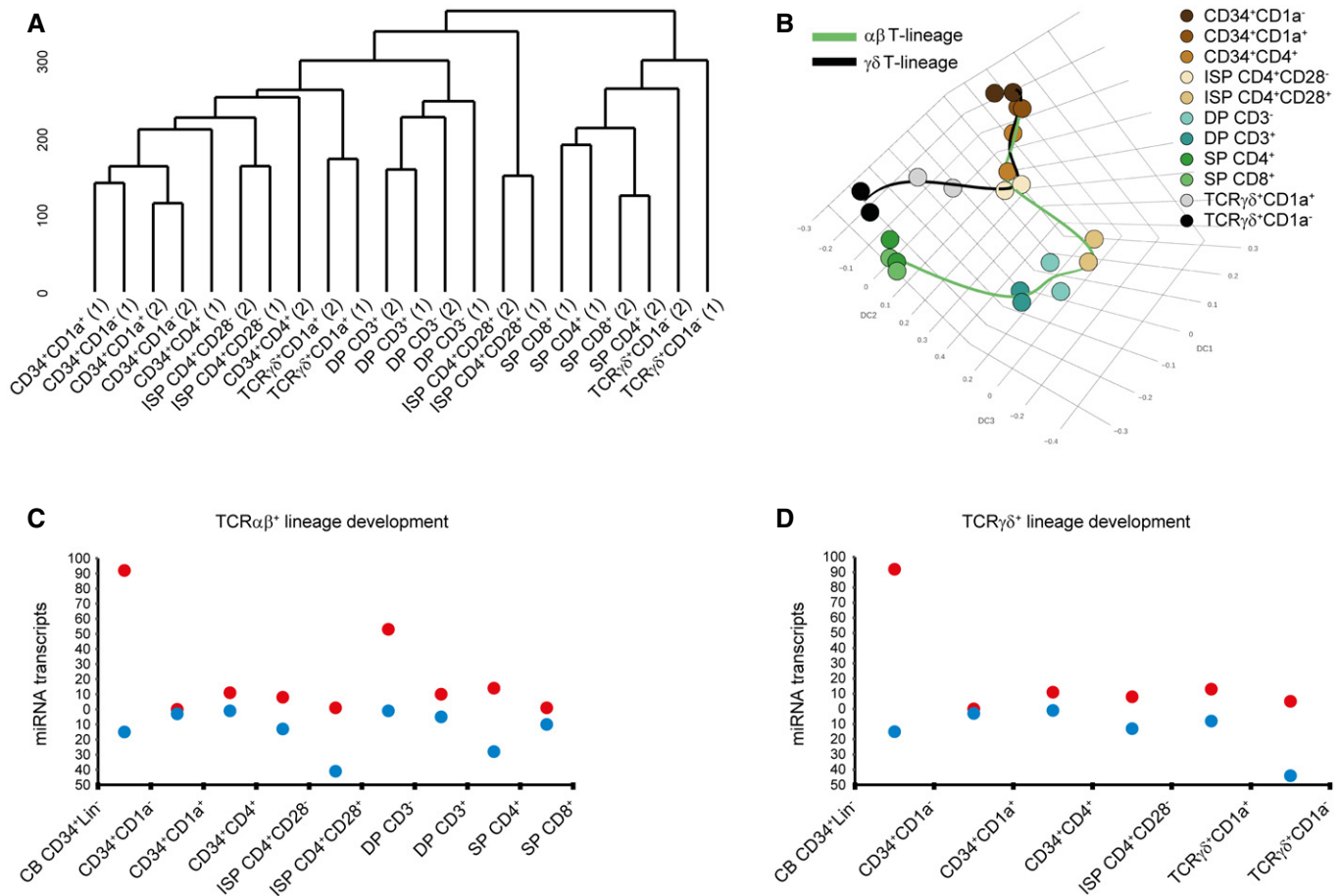


**Figure 3. Overview of the miRNA landscape across human T cell development.**

- A** Dendrogram classifying the T cell developmental subsets and replicates ( $n = 2$ ), based on the normalized miRNA expression.
- B** Diffusion map, displaying the first three DCs, generated from the miRNA expression profiles reconstructing the developmental trajectories of the  $\alpha\beta$  and  $\gamma\delta$  developmental lineages across human thymocyte subsets. The line connecting the different subsets is reflecting the developmental stages of human T cell development.
- C, D** Scatterplot displaying the up (red)- or down (blue) regulation of miRNA ( $\log_2$  fold change  $\geq 2$ ) identified by sequential pairwise comparisons starting from CB toward either the  $\alpha\beta$  (C) or the  $\gamma\delta$  (D) developmental lineages.

of a miR-17 sponge that was validated to target miR-17 binding sites in the transduced thymocytes (Appendix Fig S5), resulted in increased *BCL11B* expression (Fig 5D). Overall, these results suggest that miR-17 can target *BCL11B* expression in human thymocytes.

### Notch-dependent *BCL11B* expression alters during intrathymic development

It is well established in the mouse that induction of *BCL11B* expression in thymus immigrating precursor cells is critically dependent on Notch activation, but that it also requires additional regulatory inputs from other transcriptional regulators such as by GATA3, TCF1 (encoded by *TCF7*), and RUNX1 [39]. However, given that our data suggest that Notch signaling induces miR-17 and that miR-17 negatively impacts *BCL11B* expression, an inverse correlation between Notch activation and *BCL11B* is anticipated during human intrathymic T-lineage differentiation. To better understand this, we investigated the stage-specific changes in expression of *BCL11B* and

*HES1*, a canonical Notch target gene, during human T cell development. As expected, both genes were strongly upregulated in the most immature  $CD34^+CD1a^-$  thymocytes compared to extrathymic  $CD34^+Lin^-$  CB HPCs (Fig 6A), consistent with their Notch-dependent regulation which was confirmed in functional Notch activation experiments in  $CD34^+Lin^-$  CB HPCs (Fig 6B and Van de Walle *et al* [28] for *HES1* data). During the immature and Notch-dependent  $CD34^+$  and  $ISP4^+CD28^-$  stages prior to  $\beta$ -selection, *BCL11B* and *HES1* levels remained similar and this was also the case in  $\gamma\delta$ -lineage cells. This not only revealed a correlation between Notch activation and *BCL11B* expression during these developmental stages, but also showed that Notch activation is prolonged in developing TCR $\gamma\delta$  T cells compared to  $\alpha\beta$ -lineage DP thymocytes. Indeed, following  $\beta$ -selection, Notch activation and *HES1* levels dropped in  $\alpha\beta$ -lineage DP thymocytes. In contrast, *BCL11B* expression increased in DP thymocytes (Fig 6A, Appendix Fig S6), suggesting an inverse correlation between Notch activity and *BCL11B* expression in these developing  $\alpha\beta$ -lineage cells. Indeed, in contrast to extrathymic

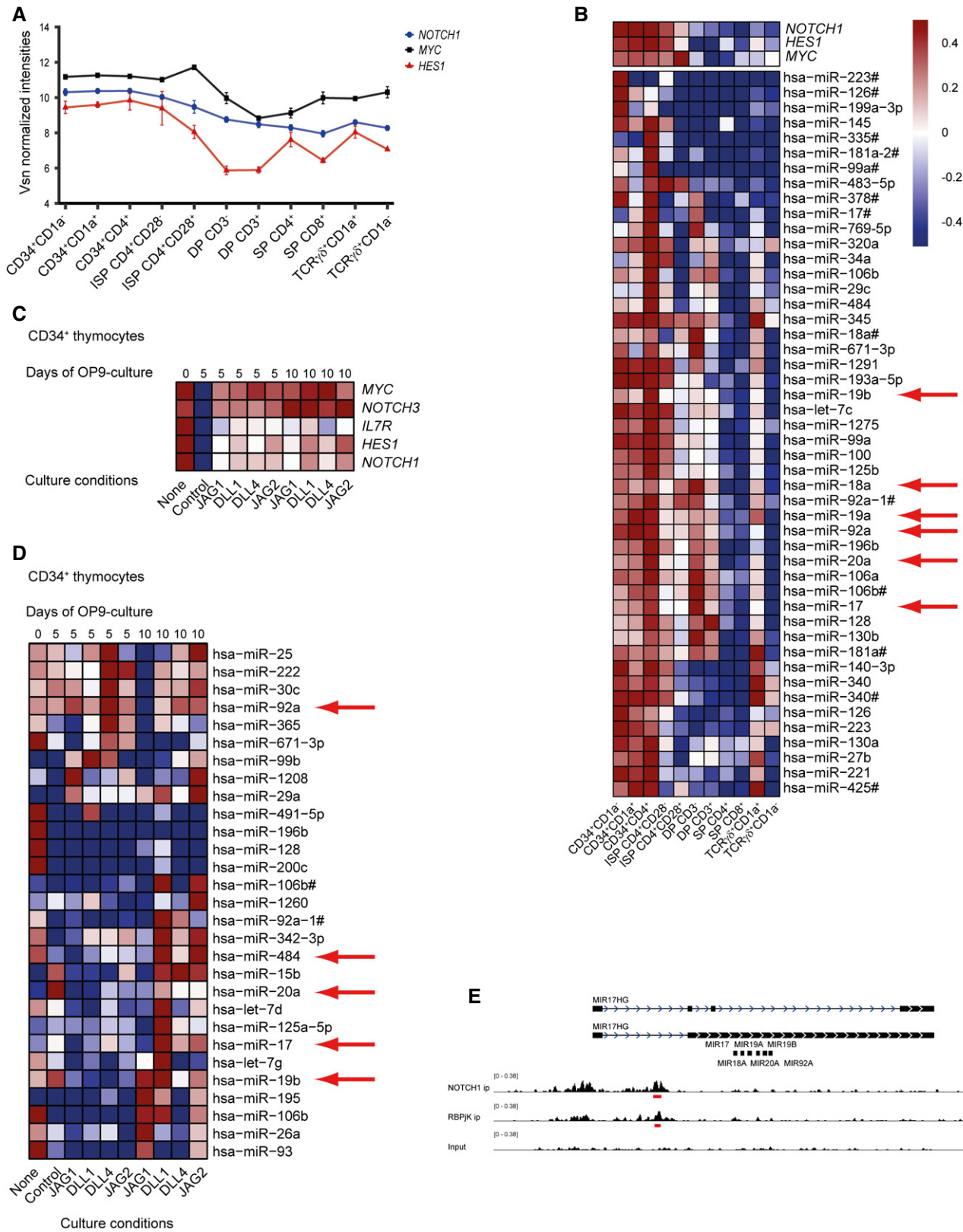


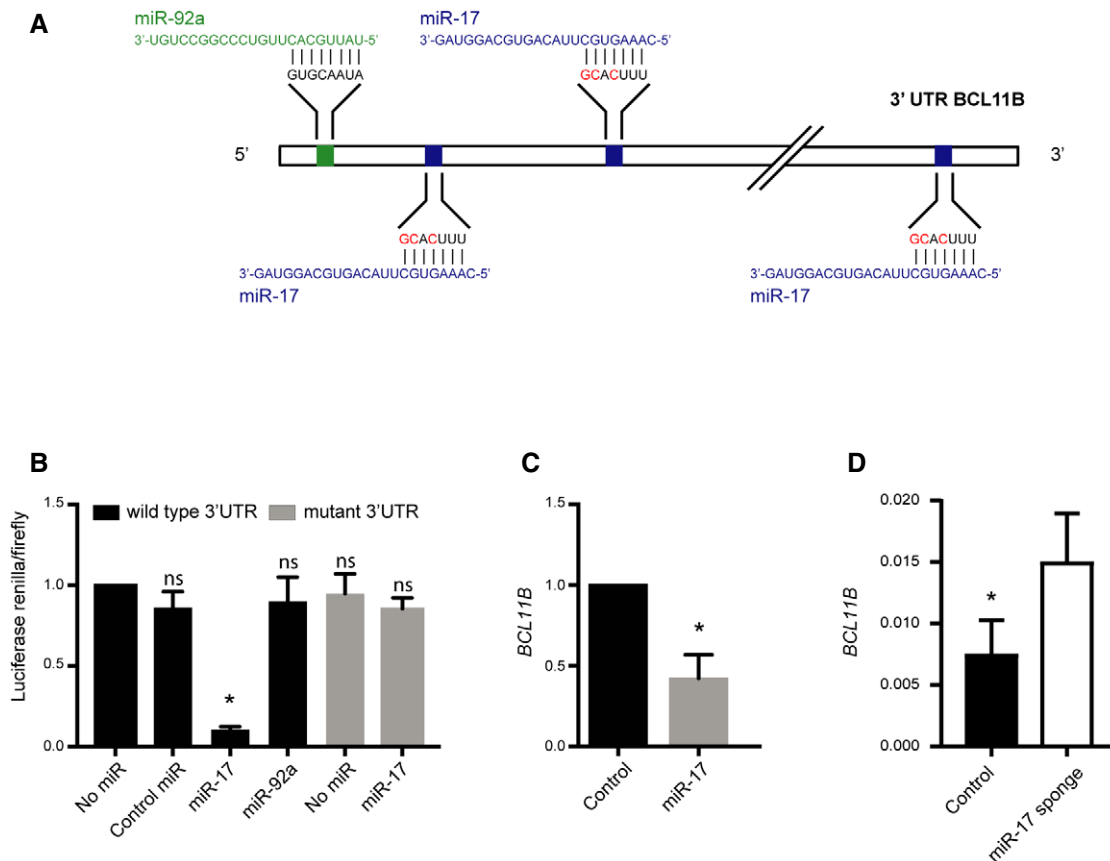
Figure 4.

**Figure 4. Notch signaling impacts the miRNA landscape in both *ex vivo* isolated as *in vitro* cultured thymocytes.**

- A Line plots displaying averaged *NOTCH1*, *MYC*, and *HES1* expression across T cell development ( $n = 2$  biological replicates; error bars indicate SEM).
- B Heatmap displaying transcript wise scaled expression of *NOTCH1*, *HES1*, *MYC*, and miRNAs from *ex vivo* isolated subsets correlating (spearman  $\rho \geq 0.5$ ) with *NOTCH1* gene expression as described in Materials and Methods. Red arrows indicate all 6 members of the miR-17–92 cluster ( $n = 2$ ).
- C Heatmap visualizing Notch1-regulated gene expression of *in vitro* cultured thymocytes across multiple culturing conditions (OP9-control, OP9-JAG1, OP9-JAG2, OP9-DLL1, and OP9-DLL4) and time points (day 0, 5, and 10).
- D *NOTCH1* correlating miRNAs (spearman  $\rho \geq 0.3$ ) of *in vitro* cultured thymocytes across multiple culturing conditions and time points. The miRNA expression levels were scaled transcript wise, and red arrows indicate members of miR-17–92 cluster ( $n = 2$ ).
- E ChIP-seq data for Notch1 and RBPj binding at the miR-17–92 locus in CUTTL1 cells. Red line underneath the ChIP-seq peaks indicates significant enrichment compared to the input sample.

CB-derived  $CD34^+Lin^-$  HPCs that upregulated *BCL11B* upon exposure to Notch activation (Fig 6B), intrathymic  $CD34^+$  precursors reduced *BCL11B* expression upon strong Notch activation (Fig 6C) and this could be rescued upon Notch inhibition using 5  $\mu$ M GSI (Fig 6D). Consistent with the proposed miR-17-mediated targeting

of *BCL11B*, miR-17 expression was not yet upregulated in Notch-exposed CB  $CD34^+Lin^-$  HPCs (Fig 6E) that activate *BCL11B* expression during the induction of T cell development (Fig 6B), and only showed Notch-dependent expression in  $CD34^+$  thymocytes that now are fully Notch-dependent (Fig 6F), consistent with

**Figure 5. Regulation of *BCL11B* expression in thymocytes through miR-17.**

- A Schematic representation of the potential miR-17 (blue) and miR-92a (green) binding sites in the 3' UTR of the *BCL11B* gene. Three nucleotides in the 3 putative miR-17 binding sites which are targeted for mutagenesis, used in a 3'UTR luciferase reporter assay described in (B), are depicted in red.
- B Transfection of miR-17 pre-miR miRNA precursor, but not of miR-92a, specifically targets the wild-type (black bars) 3' UTR of *BCL11B* in a 3'UTR luciferase reporter assay following cotransfection of HEK293T cells in comparison with the controls (transfection of no miRNA or a control miRNA). Mutation of the predicted miR-17 binding sites in the 3'UTR *BCL11B* reporter construct prevents miR-17-dependent targeting (gray bars). Graphs show mean firefly luciferase values (from 3'UTR reporter constructs) following normalization to the cotransfected control Renilla luciferase and relative to control sample without miRNA ( $n = 5$  independent experiments; error bars indicate SEM, and \* indicates  $P < 0.05$  and ns (not significant) indicates  $P > 0.05$  in a paired *t*-test).
- C Quantitative RT-PCR gene expression analysis of *BCL11B* in control (black bar)- or miR-17 (gray bar)-transduced  $CD34^+$  thymocytes after 24 h of culture on coated Fc-DLL1 plates, relative to the geometric mean of *ACTIN* and *GAPDH* and relative to the control-transduced sample ( $n = 3$  independent experiments with different donors; error bars indicate SEM, and \* indicates  $P < 0.05$  in a paired *t*-test).
- D Quantitative real-time RT-PCR gene expression analysis of *BCL11B* in control (black bar)- or miR-17 sponge (white bar)-transduced  $CD34^+$  thymocytes, relative to the geometric mean of *ACTIN* and *GAPDH* ( $n = 5$  independent experiments with different donors; error bars indicate SEM, and \* indicates  $P < 0.05$  in a paired *t*-test).



our initial correlation studies (Fig 4B and D). Since *BCL11B* is still expressed in the immature Notch-dependent stages of human T cell development, other regulatory mechanisms must counteract the miR-17-induced repression. Analogous to the mechanisms in mice [39], we observed that loss of *GATA3* and *TCF7* in CD34<sup>+</sup> thymocytes (Appendix Fig S7A and B), and of *RUNX1* in Jurkat

cells (Appendix Fig S7C), resulted in a downregulation of *BCL11B* (Fig 6G and Appendix Fig S7D), indicating that these transcription factors are positive regulators of *BCL11B* expression in immature T cell precursors, consistent with ChIP data for these factors showing binding at the *BCL11B* locus [15,37,40–43]. These findings suggest that following the initial Notch-dependent induction

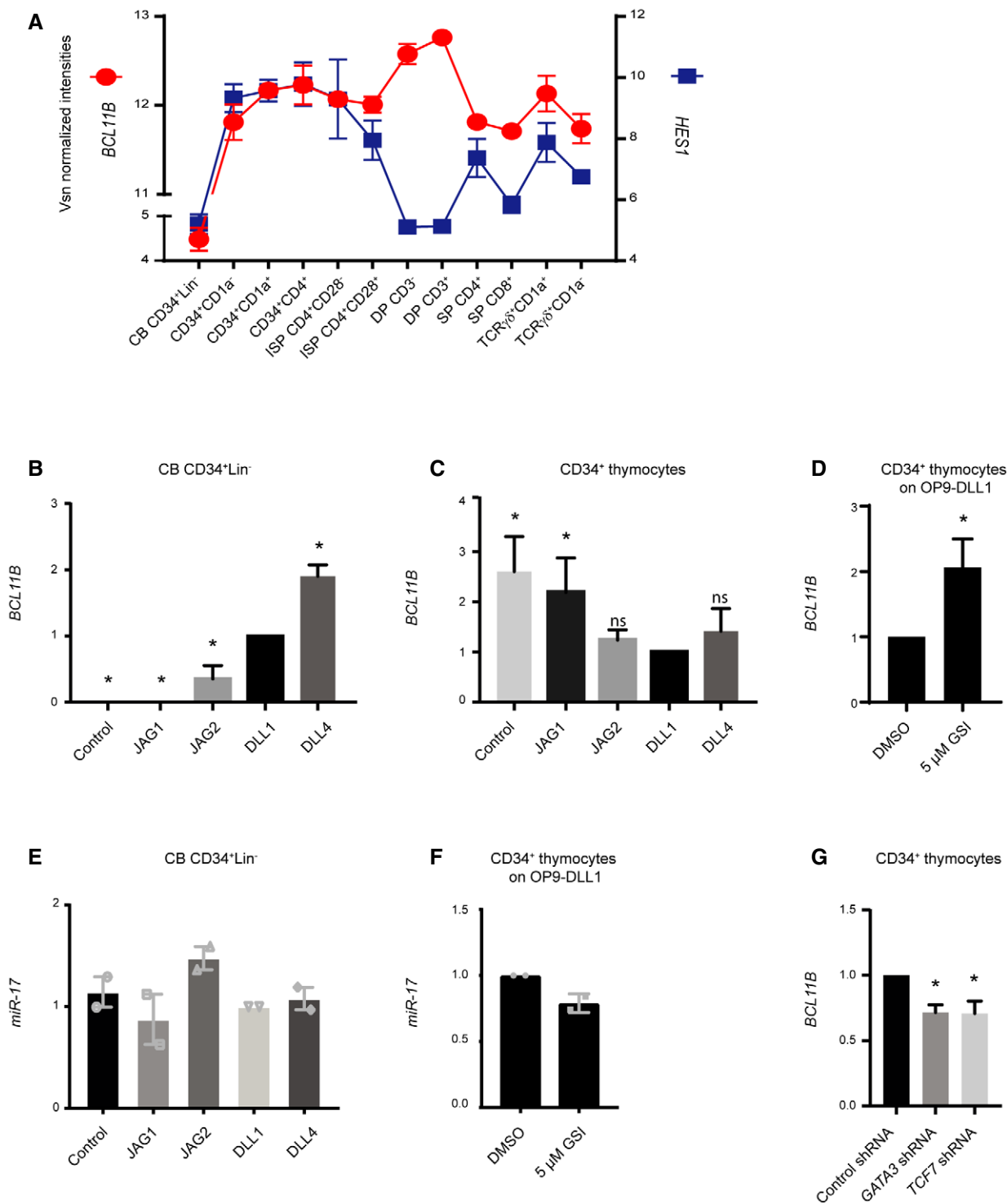


Figure 6.

**Figure 6. Notch-dependent regulation of miR-17 and BCL11B.**

- A Gene expression pattern of *BCL11B* (red dots) and *HES1* (blue squares) during human T cell development, derived from microarray data as shown in Fig 2 ( $n = 2$  biological replicates; error bars indicate SEM).
- B, C Quantitative RT-PCR expression analysis of *BCL11B* in human (B) CB CD34<sup>+</sup>Lin<sup>-</sup> and (C) CD34<sup>+</sup> thymocyte progenitors after 5 and 2 days, respectively, of coculture on OP9 stromal cells expressing different Notch ligands. Graphs show mean expression, relative to the geometric mean of *ACTIN* and *GAPDH* and relative to the OP9-DLL1 cultured cells ( $n = 4$  independent experiments with different donors; error bars indicate SEM, and \* indicates  $P < 0.05$  and ns (not significant) indicates  $P > 0.05$  in a paired  $t$ -test).
- D Quantitative RT-PCR expression analysis of *BCL11B* in human CD34<sup>+</sup> thymocyte progenitors after 2 days of coculture on OP9-DLL1 stromal cells in the presence of 5  $\mu$ M DAPT (GSI). Graphs show mean expression, relative to the geometric mean of *ACTIN* and *GAPDH* and relative to sample cultured in the presence of control DMSO ( $n = 4$  independent experiments with different donors; error bars indicate SEM, and \* indicates  $P < 0.05$  in a paired  $t$ -test).
- E, F Quantitative RT-PCR expression analysis of *miR-17* in human (E) CB CD34<sup>+</sup>Lin<sup>-</sup> and (F) CD34<sup>+</sup> thymocyte progenitors after 5 and 2 days, respectively, of coculture on (E) OP9 stromal cells expressing different Notch ligands or (F) OP9-DLL1 stromal cells in the presence of 5  $\mu$ M DAPT (GSI). Graphs show mean expression, relative to the geometric mean of *SNORD61*, *SNORD95*, and *RNU6-2* and relative to the OP9-DLL1 cultured cells (E) or to the sample cultured in the presence of control DMSO (F) ( $n = 2$  independent experiments with different donors; error bars indicate SEM—the two data points are shown).
- G Quantitative RT-PCR gene expression analysis of *BCL11B* in control (black bar)-, *GATA3* shRNA- or *TCF7* shRNA (gray bars)-transduced CD34<sup>+</sup> thymocytes after 48 h of coculture on OP9-DLL1 stromal cells, relative to the geometric mean of *ACTIN* and *GAPDH* and relative to the control-transduced sample ( $n = 6$  independent experiments with different donors for *GATA3* shRNA,  $n = 4$  independent experiments with different donors for *TCF7* shRNA; error bars indicate SEM, and \* indicates  $P < 0.05$  in a paired  $t$ -test).

of T-lineage differentiation during which *BCL11B* expression is induced, Notch activation subsequently also induces miR-17 expression that could temporally restrict higher *BCL11B* expression levels during the immature Notch-dependent stages of human T cell development and that is counteracted by positive regulators of *BCL11B*.

**miR-17 promotes human  $\gamma\delta$  T cell development**

To investigate whether miR-17 impacts human T cell development in a manner that is consistent with a role downstream of Notch1, we transduced CD34<sup>+</sup> thymocytes with a *miR-17* encoding retrovirus [44] and used the recently described artificial thymic organoid (ATO) cultures to study its impact on human T cell development [45]. In this setting, miR-17 slightly but not significantly reduced the frequencies of DP and CD3<sup>+</sup>TCR $\alpha\beta$ <sup>+</sup>  $\alpha\beta$ -lineage cells and increased the frequency of  $\gamma\delta$  T cells (Fig 7A and B). Consistent with the role of Notch1 as an important proliferation and survival factor for developing thymocytes [46], overexpression of miR-17 resulted in a significant increase in thymocyte numbers, thereby increasing DP, TCR $\alpha\beta$ , and TCR $\gamma\delta$  T cells in these cultures (Fig 7C). However, the increase was much larger for  $\gamma\delta$  T cells (28-fold) than for  $\alpha\beta$ -lineage cells (fourfold) (Fig 7C), consistent with Notch1 being more important for human  $\gamma\delta$  T cell development compared to  $\alpha\beta$ -lineage differentiation (Fig 1). The preferential development of  $\gamma\delta$  T cells compared to  $\alpha\beta$ -lineage thymocytes upon miR-17 overexpression was also confirmed in OP9-DLL4 cocultures (Fig EV3A and B). Furthermore, upon addition of 1  $\mu$ M GSI to reduce Notch activation in OP9-DLL4 cultures, miR-17 overexpression was capable of counteracting the reduction in thymocyte cellularity and most efficiently rescued  $\gamma\delta$  T cell numbers compared to those of DP and TCR $\alpha\beta$  thymocytes (Fig EV3C), consistent with the ATO cultures (Fig 7). In addition, in agreement with the observation that miR-17 can mediate Notch-driven survival and proliferation of immature thymocytes, knockdown of miR-17 (Fig EV4) resulted in an overall reduction in thymocyte cellularity (Fig EV4C), but no differential impact on the differentiation of TCR $\alpha\beta$  or TCR $\gamma\delta$  T cells was observed (Fig EV4A and B). Overall, these findings illustrate that miR-17, like Notch1, is important for the survival and/or proliferation of immature thymocytes and that miR-17 can promote

human  $\gamma\delta$  T cell development, consistent with a role downstream of Notch1.

**Higher BCL11B levels are required for human TCR $\alpha\beta$  compared to the levels for TCR $\gamma\delta$  T cell development**

To validate whether differential *BCL11B* expression levels have a functional impact on human T cell development, we performed shRNA-mediated knockdown experiments in human CD34<sup>+</sup> thymocytes that were subsequently cultured in ATOs [45]. We selected two shRNAs that induced around 50% reduction in *BCL11B* protein levels (Fig 8A) [47] which correlated with the observed difference between developing  $\gamma\delta$ - and  $\alpha\beta$ -lineage cells at both the protein (Fig 8B) and mRNA level (Fig 6A). Knockdown of *BCL11B* significantly reduced overall cellularity (Fig 8C) and the frequency of CD3<sup>+</sup>TCR $\alpha\beta$ <sup>+</sup> thymocytes (Fig 8D and E), but significantly increased the frequency of  $\gamma\delta$  T cells (Fig 8D and E). As a result, there was around a 10-fold drop in TCR $\alpha\beta$  T cells (Fig 8F) but only a 50% reduction in the number of  $\gamma\delta$  T cells (Fig 8G), resulting in an increase in the  $\gamma\delta/\alpha\beta$  T cell ratio following *BCL11B* knockdown (Fig 8H). These results therefore show that  $\alpha\beta$  T cell development is more stringently dependent on *BCL11B* compared to human  $\gamma\delta$ -lineage differentiation, consistent with the observations that Notch1 activation and miR-17 promote  $\gamma\delta$  T cell development.

**Discussion**

*BCL11B* is essential for the induction of T-lineage specification and commitment in early T cell precursors (ETPs) [23,24], as well as for the subsequent maintenance of T-lineage identity in developing thymocytes [48,49]. It was shown in mice that, in addition to the non-coding RNA ThymoD that directs the *BCL11B* enhancer-promoter interaction [50], Notch signaling, TCF1, *GATA3*, and *RUNX1* are all required in asynchronous fashion to activate *BCL11B* expression for T cell commitment, while *RUNX1* is the only factor of those that is essential to maintain *BCL11B* expression beyond that point [39]. However, the diverse subsets of mature and activated T cells that arise from these immature thymocytes, including TCR $\gamma\delta$  and TCR $\alpha\beta$  T cells [25,38], display differential expression levels and

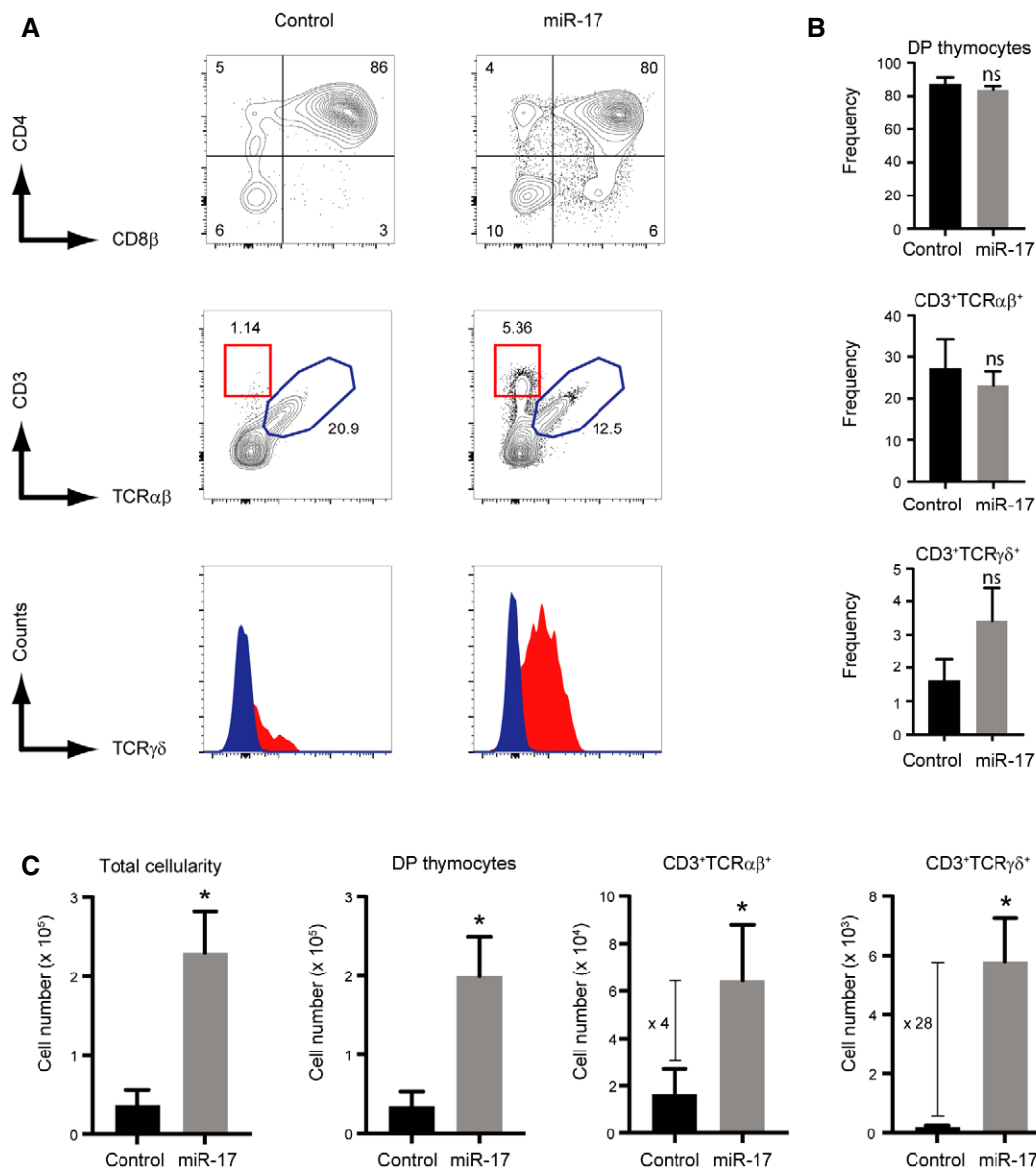


**Figure 7. Continuous miR-17 expression expands human thymocytes and enhances human TCR $\gamma\delta$  T cell development.**

A Flow cytometry analysis of control- and miR-17-transduced CD34<sup>+</sup> thymocytes, cultured in ATOs for 3 weeks. Numbers in contour plots indicate percentage of cells for the corresponding populations. Histograms show TCR $\gamma\delta$  expression in CD3<sup>+</sup>TCR $\alpha\beta$ <sup>+</sup> (blue) and CD3<sup>+</sup>TCR $\alpha\beta$ <sup>-</sup> (red) cells.

B Graphs show the mean frequency of CD4<sup>+</sup>CD8 $\beta$ <sup>+</sup> DP, CD3<sup>+</sup>TCR $\alpha\beta$ <sup>+</sup>, and CD3<sup>+</sup>TCR $\gamma\delta$ <sup>+</sup> thymocytes of control (black bar)- or miR-17 (gray bar)-transduced CD34<sup>+</sup> thymocytes in these cultures ( $n = 6$  and  $n = 8$  independent experiments for control and miR-17, respectively. Error bars indicate SEM, and ns (not significant) indicates  $P > 0.05$  in a non-parametric Mann–Whitney  $U$ -test).

C Graphs show the mean absolute cell numbers of total, CD4<sup>+</sup>CD8 $\beta$ <sup>+</sup> DP, CD3<sup>+</sup>TCR $\alpha\beta$ <sup>+</sup>, and CD3<sup>+</sup>TCR $\gamma\delta$ <sup>+</sup> thymocytes that developed in these cultures ( $n = 6$  and  $n = 8$  independent experiments for control and miR-17, respectively. Error bars indicate SEM, and \* indicates  $P < 0.05$  in a non-parametric Mann–Whitney  $U$ -test).

functions of *BCL11B*, pointing toward the requirement for additional regulatory inputs [51]. The data in this manuscript indicate that Notch activation not only activates *BCL11B* expression during human T-lineage specification and commitment, but that it shortly thereafter also may incorporate a miR-17-dependent negative feedback loop that prevents premature further upregulation of *BCL11B* until the developing thymocytes have passed the  $\beta$ -selection checkpoint when Notch activation is turned off. This would indicate that the role of Notch activation in mediating *BCL11B* expression is not

only limited as a pioneering factor to facilitate T-lineage commitment, but that it can also restrict *BCL11B* expression levels during the subsequent Notch-dependent stages of T cell development. Such a mechanism helps to explain how Notch signal strength impacts human TCR $\gamma\delta$  versus TCR $\alpha\beta$  T cell development. Based on the data in this manuscript, we propose a novel temporal and stage-specific Notch-driven mechanism through which miR-17 can restrict *BCL11B* expression during the immature Notch-dependent stages of human T cell development as schematically illustrated in Fig 9.

The Notch pathway is involved in many biological processes and involves activation of different downstream molecular regulators that integrate with lineage-specific factors to drive particular tissue

and cell type-specific molecular events. Within the hematopoietic system, Notch signaling plays distinct and lineage-specific roles, particularly during T cell development. Yet, even within this specific

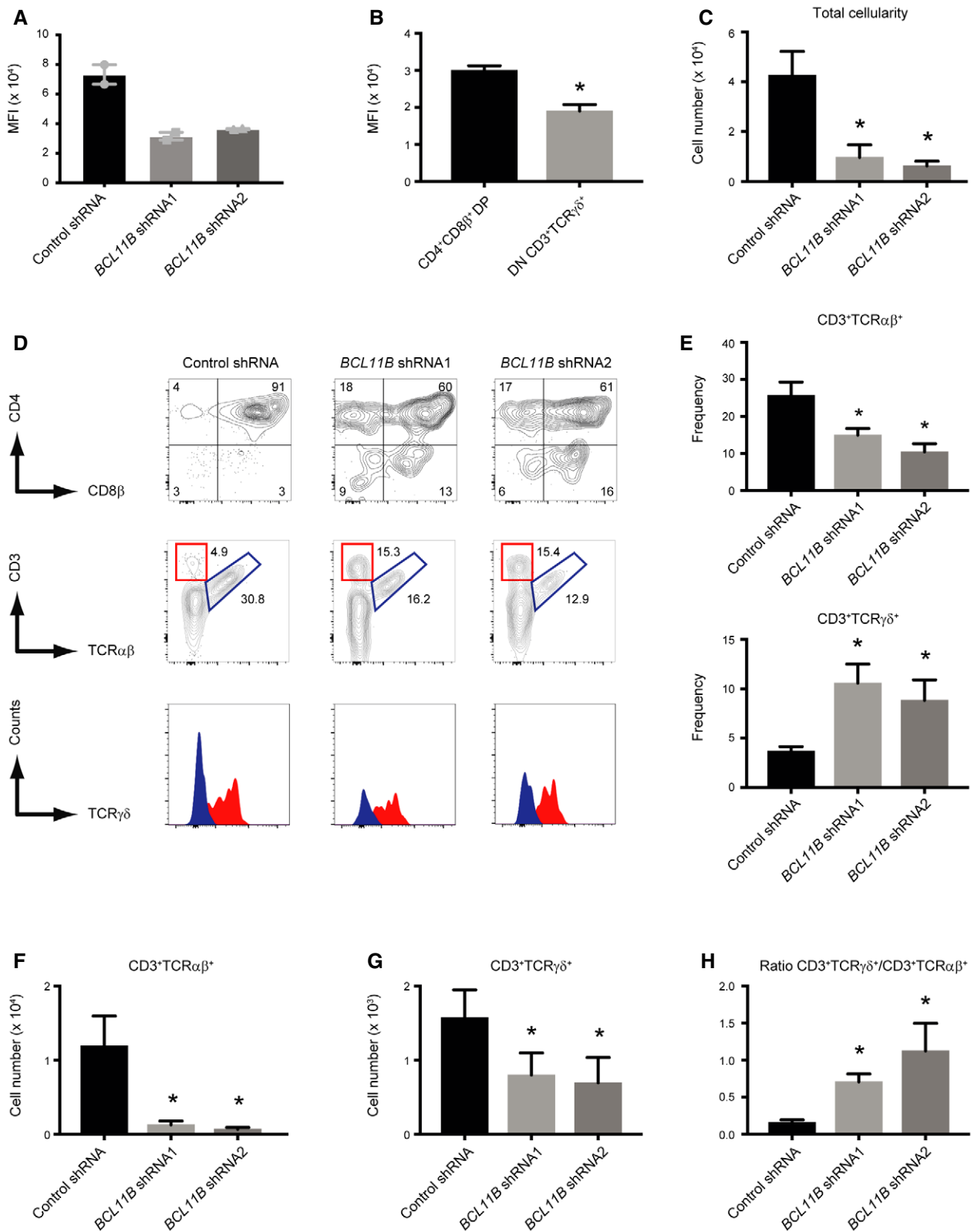


Figure 8.

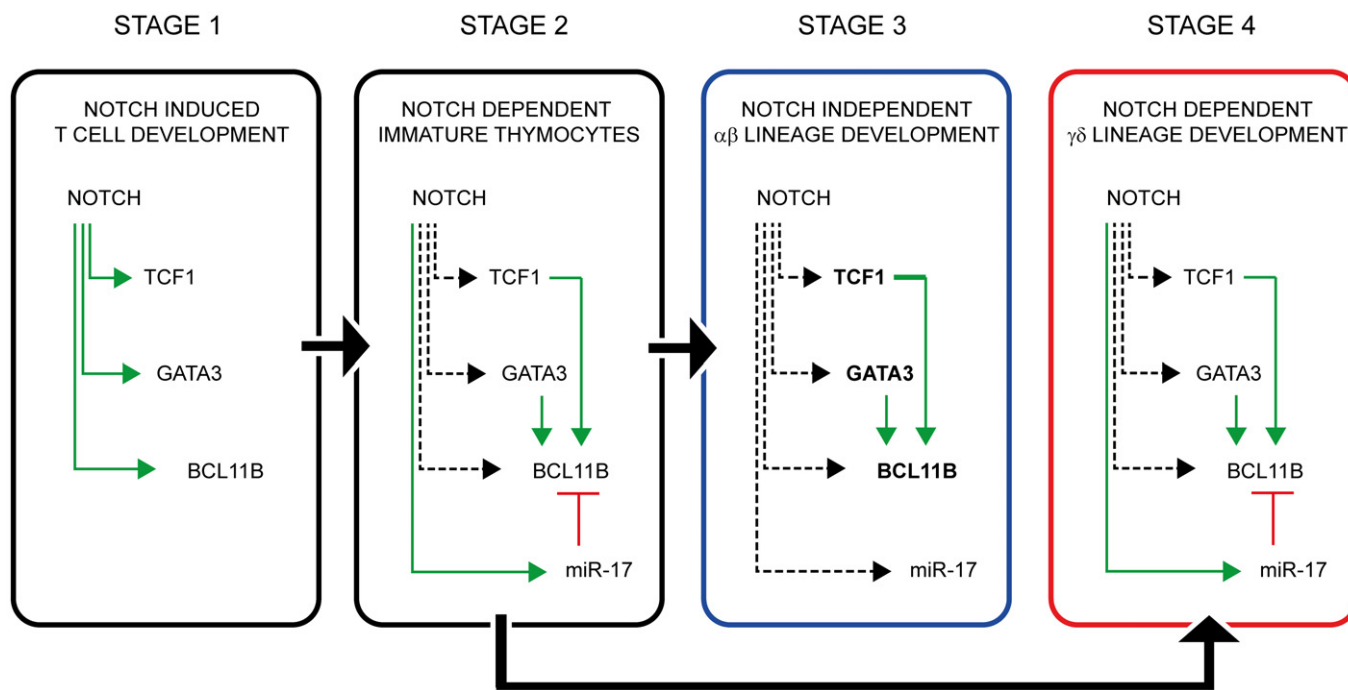


**Figure 8. Human TCR $\alpha\beta$  T cell development is more *BCL11B*-dependent compared to TCR $\gamma\delta$  T cell development.**

- A Flow cytometry analysis showing mean of median fluorescence intensity (MFI) of *BCL11B* protein levels in Jurkat cells, 72 h post-transduction with control shRNA (black bar), *BCL11B* shRNA1 or *BCL11B* shRNA2 (gray bars), each normalized to the FMO sample (*BCL11B* stained–*BCL11B* unstained sample) ( $n = 2$  independent experiments; error bars indicate SEM—the two data points are shown).
- B Flow cytometry analysis showing mean of MFI of *BCL11B* protein levels in CD4<sup>+</sup>CD8 $\beta$ <sup>+</sup> DP (black bar) and CD4<sup>-</sup>CD8 $\beta$ <sup>-</sup> DN CD3<sup>+</sup>TCR $\gamma\delta$ <sup>+</sup> (gray bar) *ex vivo* thymocytes, normalized to FMO sample (*BCL11B* stained–*BCL11B* unstained sample) ( $n = 4$  independent experiments with different donors; error bars indicate SEM, and \* indicates  $P < 0.05$  in a paired  $t$ -test).
- C Mean total cell numbers of control shRNA (black bar)-, *BCL11B* shRNA1- or *BCL11B* shRNA2 (gray bars)-transduced CD34<sup>+</sup> thymocytes, cultured in ATOs for 3 weeks ( $n = 5$  independent experiments with different donors; error bars indicate SEM, and \* indicates  $P < 0.05$  in a non-parametric paired Wilcoxon test).
- D Flow cytometry analysis of CD4<sup>+</sup>CD8 $\beta$ <sup>+</sup> DP, CD3<sup>+</sup>TCR $\alpha\beta$ <sup>+</sup> (blue), and CD3<sup>+</sup>TCR $\alpha\beta$ <sup>-</sup> (red) thymocytes that developed in corresponding cultures from (C). Numbers in contour plots indicate the percentage of cells for the corresponding populations. Histograms show TCR $\gamma\delta$  expression in CD3<sup>+</sup>TCR $\alpha\beta$ <sup>+</sup> (blue) and CD3<sup>+</sup>TCR $\alpha\beta$ <sup>-</sup> (red) cells.
- E Graphs show the mean frequency of CD3<sup>+</sup>TCR $\alpha\beta$ <sup>+</sup> and CD3<sup>+</sup>TCR $\gamma\delta$ <sup>+</sup> thymocytes that developed in these cultures ( $n = 5$  independent experiments with different donors; error bars indicate SEM, and \* indicates  $P < 0.05$  in a paired  $t$ -test).
- F, G Mean absolute cell numbers of (F) CD3<sup>+</sup>TCR $\alpha\beta$ <sup>+</sup> and (G) CD3<sup>+</sup>TCR $\gamma\delta$ <sup>+</sup> thymocytes that developed in these cultures ( $n = 5$  independent experiments with different donors; error bars indicate SEM, and \* indicates  $P < 0.05$  in a non-parametric paired Wilcoxon test).
- H CD3<sup>+</sup>TCR $\gamma\delta$ <sup>+</sup>/CD3<sup>+</sup>TCR $\alpha\beta$ <sup>+</sup> ratio from cultures depicted in (D) ( $n = 5$  independent experiments with different donors; error bars indicate SEM, and \* indicates  $P < 0.05$  in a paired  $t$ -test).

cell type, the mechanisms through which Notch signaling controls the various stages of T cell development are still unclear and quite complex. This is clearly illustrated by the asynchronous and variable expression of well-established Notch target genes that demand additional regulatory inputs [2,36,52]. Although more work is required to formally demonstrate the direct regulation of the correlated miRNAs by Notch1, our work indicates that miRNAs may serve as an additional regulatory layer through which Notch activation can induce different developmental outcomes by modifying the expression levels of their direct downstream targets. We believe that this allowed us to unravel a novel layer in the molecular mechanisms through which Notch activation drives expansion of

immature thymocytes and promotes human  $\gamma\delta$  T cell development. By including miRNAs in its pathway, Notch signaling could fulfill an indirect and negative regulatory role on *BCL11B* expression after and independent from its initial, but transient, involvement as a positive regulatory factor during the T-lineage commitment process. Thus, activation of miRNAs permits Notch signaling to function as a repressor and more subtle regulator of gene expression, in addition to its role as a direct activator. This further strengthens the idea that Notch initially serves as a pioneering factor that enables activation of critical T-lineage genes during the specification and commitment stages (Fig 9, stage 1) but for which Notch-dependent regulation becomes dispensable at later stages of T cell development, a

**Figure 9. Schematic overview of the temporal regulation of *BCL11B* expression during critical stages of human T cell development.**

Schematic representation of the proposed temporal regulation of *BCL11B* expression during critical stages of human T cell development as explained in more detail in the discussion of the manuscript.

necessary feature since Notch activation is shut down following  $\beta$ -selection [52,53].

Following the Notch1-dependent induction of T-lineage specification that is well established across species, Notch activation is particularly important for the expansion of the early pool of intrathymic T cell precursors. Our data now suggest that Notch may induce miR-17 expression at this stage of T cell development to mediate this process, and this may also involve a direct and indirect regulatory mechanism through *CMYC*, a well-established Notch target gene [54] in T-lineage cells that has been shown to regulate the miR-17–92 cluster [55]. At this point during T cell development, *BCL11B* expression is also positively regulated by other transcriptional regulators including *GATA3* and *TCF1*, that apparently are more prolonged required during human compared to during murine T cell development to drive *BCL11B* expression [39], and most likely also by *RUNX1* which is similar as in mice. These factors thus can counteract the potential negative impact of miR-17 on *BCL11B* in these Notch-dependent immature thymocytes to maintain expression of this critical transcription factor since all of these factors are coexpressed in these precursors (Fig 9, stage 2) [23,24,38,49]. Interestingly, the miR-17–92 cluster was shown to be important for IL-7 signaling in mice [56] and this is consistent with the notion that Notch1 regulates *IL7R* expression in human thymocytes [57] and the fact that IL7 is a critical growth factor for these immature thymocytes. Although no impact on  $\beta$ -selection and  $\gamma\delta$  T cell development is observed in miR-17–92-deficient mice, and also not upon miR-17 knockdown in humans in the ATO system, the increase in human  $\gamma\delta$  T cell upon miR-17 overexpression is consistent with the higher IL-7 requirement for developing  $\gamma\delta$  T cells compared to differentiating DP  $\alpha\beta$ -lineage cells which is also apparent in humans [14]. Thus, it cannot be excluded that miR-17 mediates IL-7 signaling in both mouse and humans, but that the mechanism is active at distinct stages of T cell development due to the different timing and roles of Notch activation between both species [2,25] as also further demonstrated in this manuscript. In addition, homeostatic mechanisms *in vivo* may compensate for partial phenotypes that are therefore more clearly detectable *in vitro*. Interestingly, reduced IL-7 signaling is also associated with higher *Bcl11b* expression during mouse T cell development [23], which is also consistent with our proposed antagonism between miR-17 and *BCL11B*. The lack of phenotype in the miR-17 knockdown setting may indicate that a twofold increase in *BCL11B* expression has no negative impact on  $\gamma\delta$  T cell development. In addition, the loss of miR-17 will most likely also impact the expression of other genes that may also influence this process. As such, our proposed miR-17-mediated targeting of *BCL11B* might only be part of the regulatory role of miR-17 during early human T cell development. Further studies will be required to fully understand the role of miR-17 in this process.

The Notch dependency of developing  $\alpha\beta$ -lineage cells is known to change following  $\beta$ -selection. With the exception of *CMYC* that is more prolonged required to support the proliferation of cells passing through this  $\beta$ -selection checkpoint [36], all other Notch target genes are mostly turned off [8,14,30] and further DP and SP differentiation occurs independently from Notch [9]. We have previously shown that human  $\alpha\beta$ -lineage differentiation is less stringently required on Notch activation compared to murine T cell development [2,14,30] and have extended this even further in this manuscript using Notch1 inhibition. However, low-level Notch

activation remains required since deletion of *JAG2* and *DLL4* completely abolished human T cell development, suggesting also that Notch2 and/or Notch3 can compensate for loss of Notch1 during  $\alpha\beta$ -lineage differentiation. We did observe that miR-17 is still expressed in DP thymocytes that differentiate toward the  $\alpha\beta$ -lineage which appears to be inconsistent with its potential targeting of *BCL11B* since also *BCL11B* expression levels rise in DP thymocytes. However, at that stage, *BCL11B* expression may be further enhanced by its positive regulators *GATA3* and *TCF7* that show increased expression in DP cells (Fig 9, stage 3). Thus, it is clear that during the various stages of human T cell development, *BCL11B* expression is dynamically regulated by multiple different regulatory inputs that can alter during this developmental process. The expression of miR-17 in DP thymocytes also indicates that other regulatory mechanisms besides Notch can control expression of the miR-17–92 cluster.

In contrast, human  $\gamma\delta$  T cell development, and particularly the development of immature *CD1a*<sup>+</sup>  $\gamma\delta$  T cells, remains strongly dependent on Notch activation. In this differentiation process, Notch may thus maintain *miR-17* expression to limit *BCL11B* expression that is not required for  $\gamma\delta$  development (Fig 9, stage 4). While previous work from our laboratory has demonstrated that *JAG2*-mediated Notch3 activation is important for human  $\gamma\delta$  T cell development [16], it was also clear that this interaction only partially explained the Notch-dependent development of this T cell lineage based on previous GSI experiments [14]. Consistent with the fact that Notch3 expression is dependent on initial *DLL4*-dependent Notch1 activation in ETPs and that both *DLL4* and *JAG2* can activate Notch1, we now show that inhibition of Notch1 virtually completely abolishes human  $\gamma\delta$  T cell development and that both *DLL4* and *JAG2* are important in this process in a dose-dependent manner. Besides a role in the proliferation of immature  $\gamma\delta$  T cells, it remains to be established whether Notch activation is also required for rearrangement of the *TCR $\gamma$*  and *TCR $\delta$*  loci, analogous as documented for the *TCR $\beta$*  locus in both mouse [9] and humans [58]. Nevertheless, this study further highlights the remarkable difference in Notch activation requirements between mouse and humans with respect to its role during *TCR $\gamma\delta$*  and *TCR $\alpha\beta$*  T cell development, illustrating the need for human studies to fully understand the molecular mechanism that can alter normal developmental processes and induce disease.

Indeed, the Notch/miR-17/*BCL11B* axis that we propose here and the demonstration that *BCL11B* is more stringently required for human  $\alpha\beta$ -lineage differentiation compared to  $\gamma\delta$  development help to understand the mechanisms through which some previously described hematological aberrations may have developed. In the context of T-ALL, oncogenic Notch1 activation is involved in over 60% of T-ALL cases, whereas *BCL11B* is considered to be a tumor suppressor gene [59]. Based on our work, aberrant Notch activation thus may also incorporate a miR-17-dependent mechanism that reduces expression of the *BCL11B* tumor suppressor gene. As such, activation of the miR-17–92a cluster as a result of oncogenic Notch activation can lead to multiple cooperative events that facilitate leukemogenesis [44] and this most likely also occurs in other Notch-driven cancers [60]. In addition, patients with loss-of-function *BCL11B* mutations have recently been described and are characterized by a severe depletion of conventional  $\alpha\beta$  T cells [61,62] and a relative increase in  $\gamma\delta$  T cells [61]. Our work reveals that this

phenotype most likely results from developmental aberrations during T cell development.

By incorporating the precisely defined  $\beta$ -selection checkpoint and both immature and mature intrathymic developing  $\gamma\delta$  T cell subsets, all from human postnatal thymus, our data provide significant novel insights into the molecular regulation of human T cell development since these specific stages were omitted in previous studies [31–33]. This now allows to further study the molecular drivers that mediate the TCR $\alpha\beta$  versus TCR $\gamma\delta$  lineage decision in humans and should also reveal mechanisms that are relevant for mouse  $\gamma\delta$  T cell development since this has not yet been carefully studied in this species, in contrast to  $\alpha\beta$ -lineage differentiation [36]. Furthermore, by incorporating paired mRNA/miRNA data, we provide a strong resource for further unraveling miRNA-dependent gene regulation during T cell development that is possibly also relevant in other hematopoietic lineages or other tissues.

## Materials and Methods

### Isolation of hematopoietic progenitor cells and thymocytes

Cord blood and thymus samples (obtained from children undergoing cardiac surgery) were obtained with informed consent, and all human samples were used according to the guidelines of and with the permission of the Ethical Committee of the Ghent University Hospital (Belgium) (EC UZG 2013-1168, 2019-0826). All samples were obtained with informed consent, and the experiments conformed to the principles set out in the Declaration of Helsinki and the Department of Health and Human Services Belmont Report. From CB, mononuclear cells were isolated via Lymphoprep density gradient. CD34<sup>+</sup> cells were subsequently purified by CD34 magnetic-activated cell sorting (MACS) beads (Miltenyi Biotec), according to the manufacturer's instructions. Subsequently, enriched CD34<sup>+</sup> cells from CB were labeled with CD34-APC, CD3-PE, CD14-PE, CD19-PE, and CD56-PE, and CD34<sup>+</sup>Lin<sup>-</sup> cells were sorted with a FACSAria II (BD). CD34<sup>+</sup> MACS-purified thymocytes were stained with CD34-APC, CD1a-FITC (clone OKT6, produced in-house and FITC-labeled using Molecular Probes, F-1906), and CD4-PE to sort CD34<sup>+</sup>CD1a<sup>-</sup>CD4<sup>-</sup> uncommitted (CD34<sup>+</sup>CD1a<sup>-</sup>), CD34<sup>+</sup>CD1a<sup>+</sup>CD4<sup>-</sup> (CD34<sup>+</sup>CD1a<sup>+</sup>) committed, and CD34<sup>+</sup>CD1a<sup>+</sup>CD4<sup>+</sup> (CD34<sup>+</sup>CD4<sup>+</sup>) early thymocytes. All in-house produced antibodies were used at 1  $\mu$ g per 10<sup>6</sup> cells. To obtain CD4<sup>+</sup>CD3<sup>-</sup>CD28<sup>-</sup> and CD4<sup>+</sup>CD3<sup>-</sup>CD28<sup>+</sup> cells, total thymus suspension was stained with CD3-FITC (clone OKT3, produced in-house and FITC-labeled using Molecular Probes, F-1906), CD8-FITC (clone OKT8, produced in-house and FITC-labeled using Molecular Probes, F-1906), and glycophorin (clone 10F7MN, produced in-house and used unlabeled) and antibody-labeled cells were subsequently depleted using sheep anti-mouse IgG magnetic Dynal beads (Invitrogen), according to the manufacturer's instructions. Next, depleted cells were stained with CD4-PE, CD34-FITC, CD3-FITC, CD8-FITC, and CD28-APC to sort CD4<sup>+</sup>CD34<sup>-</sup>CD3<sup>-</sup>CD8<sup>-</sup>CD28<sup>-</sup> (ISP CD4<sup>+</sup>CD28<sup>-</sup>) and CD4<sup>+</sup>CD34<sup>-</sup>CD3<sup>-</sup>CD8<sup>-</sup>CD28<sup>+</sup> (ISP CD4<sup>+</sup>CD28<sup>+</sup>) pre- and post- $\beta$ -selected thymocytes, respectively. CD4<sup>+</sup>CD8 $\beta$ <sup>+</sup>CD3<sup>-</sup> (DP CD3<sup>-</sup>) and CD4<sup>+</sup>CD8 $\beta$ <sup>+</sup>CD3<sup>+</sup> (DP CD3<sup>+</sup>) double-positive and CD4<sup>+</sup>CD3<sup>+</sup> (SP CD4<sup>+</sup>) and CD8<sup>+</sup>CD3<sup>+</sup> (SP CD8<sup>+</sup>) single-positive thymocytes were sorted following CD4-APC, CD8 $\beta$ -PECy7, and CD3-FITC labeling of total thymus cell suspension. TCR $\gamma\delta$ <sup>+</sup> cells were isolated via MACS

by labeling the thymocytes with antiTCR $\gamma\delta$  hapten antibodies and adding MACS anti-hapten FITC-labeled microBeads. Enriched TCR $\gamma\delta$ <sup>+</sup> cells were stained with CD3-PE and CD1a-PacBlue to sort CD3<sup>+</sup>TCR $\gamma\delta$ <sup>+</sup>CD1a<sup>+</sup> immature (TCR $\gamma\delta$ <sup>+</sup>CD1a<sup>+</sup>) and CD3<sup>+</sup>TCR $\gamma\delta$ <sup>+</sup>CD1a<sup>-</sup> mature (TCR $\gamma\delta$ <sup>+</sup>CD1a<sup>-</sup>) TCR $\gamma\delta$  T cells or with CD3-APC, CD1a-PacBlue, CD28-biotin, Streptavidin-PerCpCy5.5, and CD73-PE to sort TCR $\gamma\delta$ <sup>+</sup>CD3<sup>+</sup>CD28<sup>+</sup>CD1a<sup>+</sup>CD73<sup>-</sup> uncommitted and TCR $\gamma\delta$ <sup>+</sup>CD3<sup>+</sup>CD28<sup>+</sup>CD1a<sup>+</sup>CD73<sup>+</sup> committed TCR $\gamma\delta$  T cells. Purity of the isolated cells was defined on a FACSCalibur or LSRII (BD) and was always > 98%.

### RNA isolation, miRNA profiling, and gene expression analysis

RNA extraction was performed using the miRNeasy Mini or Micro Kit (Qiagen). The RNA yield was determined by NanoDrop technology (Thermo Fisher Scientific), and quality was verified on the Agilent 2100 bioanalyzer (Agilent Technologies). Whole human genome expression profiling was performed using the GeneChip Human Genome U133 2.0 Plus arrays (Affymetrix), according to standardized procedures at the IGBMC ([www.igbmc.fr](http://www.igbmc.fr)). The expression of 756 miRNAs and 3 small RNA controls was determined using the TaqMan stem-loop RT-qPCR method as previously described [44,63]. All gene expression profiling data have been deposited in the GEO database (GSE71753). For quantitative RT-PCR of mRNA, RNA was converted into cDNA using Superscript RT II (Invitrogen) or iScript Advanced RT (Bio-Rad), according to the manufacturer's instructions. Real-time PCRs were performed using the LightCycler 480 SYBR Green I Master Mix (Roche) using primers targeting *BCL11B*, *GATA3*, *TCF7*, *RUNX1*, *ACTIN*, or *GAPDH*. Relative expression levels of *BCL11B*, *GATA3*, *TCF7*, or *RUNX1* were calculated using *ACTIN* and *GAPDH* for normalization. Primer sequences are described in Appendix Table S1. For quantitative RT-PCR of miR-17, RNA was converted into cDNA using miScript II RT (Qiagen), according to the manufacturer's instructions. Real-time PCRs were performed using the miScript SYBR Green Master Mix (Qiagen) using miScript Universal Primer in combination with miScript Primer assay (Qiagen) containing a forward primer targeting *miR-17*, *SNORD61*, *SNORD95*, and *RNU6-2*, according to the manufacturer's instructions. Relative expression level of *miR-17* was calculated using *SNORD61*, *SNORD95*, and *RNU6-2* for normalization.

### Microarray and miRNA data analysis

For both the microarray data obtained from *ex vivo* sorted and cocultured samples, vsn normalization was performed with the vsnrma package. Annotation of the probes was performed with the biomaRt package. The miRNA data for both the *ex vivo* and coculture datasets were normalized according to the global mean normalization [64]. Briefly, Cq values above 32 were removed and samples were mean centered. Next, miRNAs expressed in less than two samples were removed and missing values were imputed by the highest value for each miRNA. Lastly, the entire matrix was multiplied by -1 allowing for visual comparison with the microarray data.

Pairwise comparisons between biological replicates for each subset in both the *ex vivo* sorted microarray and miRNA datasets were used to assess global systematic differences across transcripts. This quality control was accompanied by the R-squared to aid visual

assessment of the quality. In order to obtain up- and downregulated genes and miRNAs, expression levels were averaged across biological replicates for both the mRNA and miRNA datasets. Subsequently,  $\log_2$  fold changes were obtained by subtracting averaged  $\log_2$  normalized expression during pairwise comparisons.

Development across developmental stages was assessed by both diffusion maps and dendrograms. For both the mRNA and miRNA datasets obtained from the *ex vivo* sorted thymocyte subsets, the normalized matrices were used to generate diffusion maps. Diffusion maps were made with the destiny package. Similarly as for the diffusion maps, the normalized matrices were used to generate dendrograms. For the mRNA and miRNA datasets, the Euclidean distance with ward.D linkage and Manhattan distance with average linkage measure were used, respectively.

Correlation analysis was performed on both the *ex vivo* and *in vitro* cultured miRNA datasets. The Notch1 probe representing the highest overall expression was retained from either the *ex vivo* sorted or the *in vitro* cultured mRNA dataset and used to assess correlation with either the *ex vivo* sorted or the *in vitro* cultured miRNA datasets, respectively. Spearman correlation was used to assess positive correlation. The miRNAs with a correlation  $> 0.5$  or  $0.3$ , for the *ex vivo* sorted or *in vitro* cultured miRNA datasets respectively, were retained. Finally, the retained miRNAs were rescaled independently of each other. This allows visualization of subtle differences in expression patterns, but hinders comparison between miRNAs.

### Fetal thymus organ cultures

Fetal thymus organ cultures were performed as described [26]. All animals were treated and used according to the guidelines and with the permission of the Animal Ethical Commission of Ghent University Hospital. NOD-LtSz-scid/scid (NOD/SCID) mice (originally purchased from The Jackson Laboratory) were obtained from our own specific pathogen-free breeding facility. Fetal thymic lobes from these mice were isolated at fetal days 14–15 of gestation, and 10,000 human progenitors were added to each lobe in 2 days hanging drop cultures in medium containing 20  $\mu\text{g}/\text{ml}$  isotype control or anti-Notch1 blocking antibody [65]. Lobes were transferred to FTOC in medium containing 15  $\mu\text{g}/\text{ml}$  isotype control or anti-Notch1 blocking antibody. Half of the medium was refreshed every 3–4 days. To perform FTOCs with *Jag1*<sup>-</sup>, *Jag2*<sup>-</sup>, and/or *Dll4*-deficient fetal thymic lobes, homozygous *Jag1*<sup>lox/lox</sup> mice [66] and *Jag2*<sup>lox/lox</sup>*Dll4*<sup>lox/lox</sup> mice (generated by intercrossing *Jag2*<sup>lox/lox</sup> [67] and *Dll4*<sup>lox/lox</sup> mice [4]) were crossed to *Foxn1-Cre* mice (gift from N. Manley, University of Georgia, Athens, GA; [68]) to generate *Jag1*<sup>wt/lox</sup>*Foxn1-Cre*<sup>+/-</sup> mice and *Jag2*<sup>wt/lox</sup>*Dll4*<sup>wt/lox</sup>*Foxn1-Cre*<sup>+/-</sup> mice, respectively. These animals were subsequently backcrossed to the homozygous floxed mice to obtain *Jag1*<sup>lox/lox</sup>*Foxn1-Cre*<sup>-/-</sup> and *Jag1*<sup>lox/lox</sup>*Foxn1-Cre*<sup>+/-</sup> mice, as well as *Jag2*<sup>lox/lox</sup>*Dll4*<sup>wt/lox</sup>*Foxn1-Cre*<sup>-/-</sup>, *Jag2*<sup>wt/lox</sup>*Dll4*<sup>wt/lox</sup>*Foxn1-Cre*<sup>+/-</sup>, *Jag2*<sup>lox/lox</sup>*Dll4*<sup>wt/lox</sup>*Foxn1-Cre*<sup>+/-</sup>, *Jag2*<sup>wt/lox</sup>*Dll4*<sup>lox/lox</sup>*Foxn1-Cre*<sup>+/-</sup>, and *Jag2*<sup>lox/lox</sup>*Dll4*<sup>lox/lox</sup>*Foxn1-Cre*<sup>+/-</sup> mice. Fetuses from these backcrossings were isolated at fetal days 15–15.5 of gestation, and fetal thymic lobes were treated for 5 days with 1.35 mM 2'-deoxyguanosine to remove all endogenous mouse thymocytes [16]. From these fetuses, fetal liver was used for genotyping. Subsequently, 10,000 human CD34<sup>+</sup> thymocytes were added to each lobe in 2 days hanging drop cultures, before further culture as described above for FTOC.

FTOCs were performed at 37°C in a humidified atmosphere containing 7% (v/v) CO<sub>2</sub> in air. At indicated time point, cells were harvested by disrupting thymic lobes mechanically with a tissue grinder to obtain a single cell suspension that was used for flow cytometry.

### Coculture experiments

Purified progenitors were seeded onto confluent layers of OP9 stromal cells expressing specific Notch ligands, as described previously [28]. OP9 cocultures were performed in minimum essential medium alpha (MEM $\alpha$ , powder derived) containing 100 IU/ml penicillin, 100  $\mu\text{l}/\text{ml}$  streptomycin, 2 mM L-glutamine, and 20% FCS and supplemented with FLT3-L, SCF, and IL-7 (5 ng/ml each). For  $\gamma$ -secretase inhibition (GSI) experiments, various concentrations (0.2–5  $\mu\text{M}$ ) of N-[N-(3,5-Difluorophenacetyl)-L-alanyl]-S-phenylglycine t-butyl ester (DAPT, Peptides International, Louisville, KY), diluted in dimethyl sulfoxide (DMSO), were added as indicated and an equal concentration of DMSO was used as control. Cocultures were performed in 24 wells at 37°C in a humidified atmosphere containing 7% (v/v) CO<sub>2</sub> in air. At indicated time point, cells were harvested by pipetting and analyzed by flow cytometry.

### Artificial thymic organoid cultures

Artificial thymic organoid cultures were performed as described [45] with the exception that MS5-DLL4 stromal cells were used instead of MS5-DLL1 cells. MS5-DLL4 stromal cells were generated by retroviral transduction of MS5 stromal cells [26] with a DLL4 encoding retrovirus, similar as previously used for generating OP9-DLL4 stromal cells [28]. Thymocyte precursors and MS5-DLL4 stromal cells were both collected in Roswell Park Memorial Institute (RPMI) 1640 medium containing 4% B-27, 30  $\mu\text{M}$  ascorbic acid, 1% penicillin/streptomycin, and 1% GlutaMAX (R-B27 medium), supplemented with IL7 and FLT3-L (5 ng/ml) (complete ATO medium). Per ATO, 7,500 human progenitor cells were combined with 150,000 MS5-DLL4 stromal cell single cell suspension (1:20 human progenitor cell:stromal cell ratio). Mixed human progenitor cells:MS5-DLL4 stromal cells were centrifuged and subsequently resuspended in ~5  $\mu\text{l}$  complete ATO medium per ATO, which was transferred to a single cell culture insert in a 6 well containing 1 ml of complete ATO medium. Medium was refreshed every 3–4 days. ATO cultures were performed at 37°C in a humidified atmosphere containing 5% (v/v) CO<sub>2</sub> in air. At indicated time point, cells were harvested by disrupting ATOs by forceful pipetting to obtain a single cell suspension that was used for flow cytometry.

### Lenti- and retroviral transduction of human thymocyte progenitors and human T-ALL cell lines

CD34<sup>+</sup> thymocytes were pre-cultured in Iscove's modified Dulbecco's medium (IMDM) containing 100 IU/ml penicillin, 100  $\mu\text{l}/\text{ml}$  streptomycin, 2 mM L-glutamine, and 10% FCS (IMDM complete) and supplemented with SCF and IL-7 (5 ng/ml). After 24 h, cells were transduced with an equal volume of the appropriate retro- or lentiviruses using RetroNectin-coated (24  $\mu\text{g}/\text{ml}$ ) 24- or 96-well tissue culture (non-treated) plates to which additional cytokines were added to keep the concentration constant. Forty-eight h



after transduction, cells were sorted for EGFP<sup>+</sup> and used for specific assays as described in the text.

The Jurkat human T-ALL cell line (ATCC) was cultured in IMDM complete and was transduced with an equal volume of the appropriate lentiviruses using RetroNectin-coated (24 µg/ml) 24- or 96-well tissue culture (non-treated) plates. Seventy-two h after transduction, cells were sorted for EGFP<sup>+</sup> and used for flow cytometry analysis.

### Monoclonal antibodies and flow cytometry

Cell suspensions obtained from cocultures, FTOCs, and ATO cultures were first blocked with anti-mouse FcγII/III (clone 2.4.G2) and human IgG (FcBlock; Miltenyi) to avoid non-specific binding. Total thymus cell suspension or cells obtained from transduced cell sorting were blocked with anti-human IgG. Subsequently, cells were stained with combinations of anti-human monoclonal antibodies as indicated. Intracellular staining of BCL11B was performed, after initial cell surface staining if indicated, using purified rat anti-human BCL11B antibody (BioLegend) in combination with goat anti-rat IgG Alexa Fluor 647 (BioLegend) and the eBioscience™ Foxp3/Transcription Factor Staining Buffer Set (Thermo Fisher Scientific), according to the manufacturer's instructions. Fluorescence Minus One (FMO) samples were treated as described above, but without antibodies for intracellular staining.

### Viral constructs and virus production

MISSION SHC002 (control shRNA), TRCN0000033480 (Clone ID: NM\_022898.1-679s1c1) and TRCN0000033483 (Clone ID: NM\_022898.1-1836s1c1) (*BCL11B* shRNA1 and *BCL11B* shRNA2, respectively), TRCN0000019301 (Clone ID: NM\_002051.1-1231s1c1) (*GATA3* shRNA) [15], TRCN0000021674 (*TCF7* shRNA), TRCN0000338427 (Clone ID: NM\_001754.4-646s21c1), and TRCN0000338490 (Clone ID: NM\_001754.4-949s21c1) (*RUNX1* shRNA1 and *RUNX1* shRNA2, respectively) lentiviral vectors were purchased from Sigma in which the puromycin resistance gene was replaced with a PCR-amplified enhanced green fluorescent protein (EGFP) cDNA using BamHI and KpnI restriction sites (Appendix Fig S8A). Infectious lentiviral particles were produced using *TransIT*-Lenti Transfection Reagent (Mirus Bio) in combination with the HEK293FT cell line (ATCC) and one of the MISSION vectors (2 µg target DNA), in conjunction with the pCMV-VSV-G (0.2 µg envelope DNA) and p8.91 (1.8 µg packaging DNA) constructs, according to the manufacturer's instructions. The virus supernatant was harvested 48 h and 72 h after transfection. The miR-17 pre-miRNA was cloned into the MSCV-PIG (puromycin IRES GFP) vector, upstream of the PGK promoter in order to avoid miRNA-driven degradation of EGFP (Appendix Fig S8B), as described previously [44]. The empty MSCV-PIG vector was used as control.

The miR-17 sponge construct was designed according to Mullokandov et al [69]. In brief, a gBlock Gene Fragment (IDT) was designed containing cDNA coding for blue fluorescent protein (BFP) followed by 6 tandem copies of the miR-17 target sequence (5'-GCACTTTA-3'), each separated by a spacer. The restricted gBlock was cloned into the LZRS-PGK-EGFP retroviral vector (generated in-house by cloning PGK-EGFP, isolated from pRRLSIN.cPPT.PGK-GFP.WPRE (a gift from Didier Trono (Addgene plasmid # 12252; <http://n2t.net/addgene:12252>; RRID:Addgene\_12252)), into the

LZRS backbone [26] using EcoRI and XhoI restriction sites). Control sponge vector was generated by removing the tandem miR-17 target sequence from the miR-17 sponge vector using BstBI restriction. BFP is functioning as transcriptionally linked reporter for miR-17 downmodulation, EGFP as a reporter for genomic integration of the construct (Appendix Fig S8C).

Infectious retroviral particles were produced using calcium phosphate-mediated transfection (Invitrogen) of Phoenix-A cells (ATCC) with one of the retroviral vectors (10 µg target DNA), according to the manufacturer's instructions. After 14 days of puromycin selection (2 µg/ml) for positive transfected cells, the virus supernatant was harvested. Validation of all constructs was confirmed by sequence analysis prior to virus production.

### Luciferase reporter assay

The 3'UTR *BCL11B* luciferase reporter vector was generated by cloning 3'UTR *BCL11B* sequence, amplified from genomic DNA, into the psi-CHECK-2 vector (Promega) (wild-type 3'UTR *BCL11B*). Using the online target prediction program TargetScanHuman 7.0 ([www.targetscan.org](http://www.targetscan.org)), 3 putative miR-17 and 1 putative miR-92a target sites were identified in the 3' UTR of *BCL11B* (at position 658–664, 1,376–1,383, 4,626–4,632 and at position 213–220, respectively). The miR-17 predicted target sites (5'-GCACUUU-3') were mutated one by one into 5'-CGAGUUU-3' using site-directed mutagenesis through PCR with the corresponding mutagenesis primers (Appendix Table S2). After 3 PCR mutagenesis rounds, single, double, and triple mutants of the hsa-miR-17-5p target sites were obtained (mutant 3'UTR *BCL11B*). All constructs were fully sequenced to confirm wild-type and mutated 3'UTR of *BCL11B* and to exclude additional mutations. For the 3'UTR luciferase assays, HEKT cells were cotransfected with either 100 ng wild-type or mutant 3'UTR *BCL11B* luciferase reporter plasmid, in conjunction with 25 µM control miR, miR-17 pre-miR miRNA precursor, or miR-92a pre-miR miRNA precursor (Ambion) and 20 ng pRL-TK-Renilla normalizing reporter plasmid (Promega), using calcium phosphate-mediated transfection, according to the manufacturer's instructions. After 48h, luciferase activity was measured in cell lysates using a dual luciferase reporter system (Promega), according to the manufacturer's instructions.

### Statistical analysis and software

Flow cytometry data were analyzed using BD FACSDiva software or FlowJo v10. Paired *t*-tests (two-tailed), non-parametric paired Wilcoxon tests (two-tailed), and Mann–Whitney *U*-tests (two-tailed) were performed using GraphPad Prism or SPSS 24 software. The microarray and miRNA data were analyzed in R3.5.1. For both the microarray and the miRNA data, 2 biological replicates were generated. Normalization of either the microarray data or the miRNA data was performed by applying vsn or global mean normalization, respectively. For both datasets, dimensionality reduction was attained by generation of a diffusion map. Additionally, the similarity of biological replicates was determined by assessing the R-squared. Spearman's rho was determined during correlation analysis. Finally, dendrograms were generated with either Euclidean distance and ward.D linkage or Manhattan distance combined with

the average linkage measure for either the microarray or the miRNA dataset, respectively.

## Data availability

The datasets produced in this study are available in the following databases: mRNA and miRNA profiling: Gene Expression Omnibus GSE71753 (<https://www.ncbi.nlm.nih.gov/geo/query/acc.cgi?acc=GSE71753>).

**Expanded View** for this article is available online.

## Acknowledgements

The authors thank Chris Siebel (Genentech) for providing the Notch1 blocking antibody, Ute Koch and Freddy Radtke (EPFL), Thomas Gridley (Maine Medical Research Institute) and Nancy Manley (University of Georgia) for providing Dll4, Jag2, and FoxN1Cre mice, JuanCarlos Zuniga-Pflucker (University of Toronto) for OP9 stromal cells, the Ghent University Hospital Animal Facility for animal care, Dr. Katrien Francois and Dr. Guido Van Nooten (Department of Cardiac Surgery UZ Gent) for thymus tissue, and Dr Conny Matthys (Navelstrengbloedbank UZ Gent) for CB samples. This work was supported by grants of the Fund for Scientific Research Flanders (FWO), the Concerted Research Action of Ghent University (GOA), and the Foundation against Cancer (STK).

## Author contributions

A-CD: performed experiments, analyzed data, and wrote the manuscript; KD and ML: analyzed data and wrote the manuscript; JVM: performed experiments and analyzed data; IV, JDM, KW, and KDM: performed experiments; JR, P-JV, and KDP: analyzed data; TK, BV, GL, and JV: provided reagents and analyzed data; PM, PVV, and FS: provided reagents and designed research; and TT: designed research, analyzed data, and wrote the manuscript.

## Conflict of interest

The authors declare that they have no conflict of interest.

## References

- De Obaldia ME, Bhandoola A (2015) Transcriptional regulation of innate and adaptive lymphocyte lineages. *Annu Rev Immunol* 33: 607–642
- Taghon T, Waegemans E, Van de Walle I (2012) Notch signaling during human T cell development. *Curr Top Microbiol Immunol* 360: 75–97
- Hozumi K, Mailhos C, Negishi N, Hirano K, Yahata T, Ando K, Zuklys S, Hollander GA, Shima DT, Habu S (2008) Delta-like 4 is indispensable in thymic environment specific for T cell development. *J Exp Med* 205: 2507–2513
- Koch U, Fiorini E, Benedito R, Besseyrias V, Schuster-Gossler K, Pierres M, Manley NR, Duarte A, Macdonald HR, Radtke F (2008) Delta-like 4 is the essential, nonredundant ligand for Notch1 during thymic T cell lineage commitment. *J Exp Med* 205: 2515–2523
- Radtke F, Wilson A, Stark G, Bauer M, van Meerwijk J, MacDonald HR, Aguet M (1999) Deficient T cell fate specification in mice with an induced inactivation of Notch1. *Immunity* 10: 547–558
- Ciofani M, Knowles GC, Wiest DL, von Boehmer H, Zuniga-Pflucker JC (2006) Stage-specific and differential notch dependency at the alpha-beta and gammadelta T lineage bifurcation. *Immunity* 25: 105–116
- Garbe AI, Krueger A, Gounari F, Zuniga-Pflucker JC, von Boehmer H (2006) Differential synergy of Notch and T cell receptor signaling determines alphabeta versus gammadelta lineage fate. *J Exp Med* 203: 1579–1590
- Taghon T, Yui MA, Pant R, Diamond RA, Rothenberg EV (2006) Developmental and molecular characterization of emerging beta- and gamma-delta-selected pre-T cells in the adult mouse thymus. *Immunity* 24: 53–64
- Wolfer A, Bakker T, Wilson A, Nicolas M, Ioannidis V, Littman DR, Lee PP, Wilson CB, Held W, MacDonald HR, et al (2001) Inactivation of Notch 1 in immature thymocytes does not perturb CD4 or CD8T cell development. *Nat Immunol* 2: 235–241
- Dervovic DD, Liang HC, Cannons JL, Elford AR, Mohtashami M, Ohashi PS, Schwartzberg PL, Zuniga-Pflucker JC (2013) Cellular and molecular requirements for the selection of in vitro-generated CD8 T cells reveal a role for Notch. *J Immunol* 191: 1704–1715
- Doerfler P, Shearman MS, Perlmutter RM (2001) Presenilin-dependent gamma-secretase activity modulates thymocyte development. *Proc Natl Acad Sci USA* 98: 9312–9317
- Hadland BK, Manley NR, Su D, Longmore GD, Moore CL, Wolfe MS, Schroeter EH, Kopan R (2001) Gamma-secretase inhibitors repress thymocyte development. *Proc Natl Acad Sci USA* 98: 7487–7491
- Robey E, Chang D, Itano A, Cado D, Alexander H, Lans D, Weinmaster G, Salmon P (1996) An activated form of Notch influences the choice between CD4 and CD8 T cell lineages. *Cell* 87: 483–492
- Van de Walle I, De Smet G, De Smedt M, Vandekerckhove B, Leclercq G, Plum J, Taghon T (2009) An early decrease in Notch activation is required for human TCR-alphabeta lineage differentiation at the expense of TCR-gammadelta T cells. *Blood* 113: 2988–2998
- Van de Walle I, Dolens AC, Durinck K, De Mulder K, Van Loocke W, Damle S, Waegemans E, De Medts J, Velghe I, De Smedt M, et al (2016) GATA3 induces human T cell commitment by restraining Notch activity and repressing NK-cell fate. *Nat Commun* 7: 11171
- Van de Walle I, Waegemans E, De Medts J, De Smet G, De Smedt M, Snaauwaert S, Vandekerckhove B, Kerre T, Leclercq G, Plum J, et al (2013) Specific Notch receptor-ligand interactions control human TCR-alphabeta/gammadelta development by inducing differential Notch signal strength. *J Exp Med* 210: 683–697
- Haks MC, Lefebvre JM, Lauritsen JP, Carleton M, Rhodes M, Miyazaki T, Kappes DJ, Wiest DL (2005) Attenuation of gammadeltaTCR signaling efficiently diverts thymocytes to the alphabeta lineage. *Immunity* 22: 595–606
- Hayes SM, Li L, Love PE (2005) TCR signal strength influences alphabeta/gammadelta lineage fate. *Immunity* 22: 583–593
- Kreslavsky T, Garbe AI, Krueger A, von Boehmer H (2008) T cell receptor-instructed alphabeta versus gammadelta lineage commitment revealed by single-cell analysis. *J Exp Med* 205: 1173–1186
- Ciofani M, Zuniga-Pflucker JC (2010) Determining gammadelta versus alphabeta T cell development. *Nat Rev Immunol* 10: 657–663
- Lauritsen JP, Wong GW, Lee SY, Lefebvre JM, Ciofani M, Rhodes M, Kappes DJ, Zuniga-Pflucker JC, Wiest DL (2009) Marked induction of the helix-loop-helix protein Id3 promotes the gammadelta T cell fate and renders their functional maturation Notch independent. *Immunity* 31: 565–575
- Lee SY, Stadanlick J, Kappes DJ, Wiest DL (2010) Towards a molecular understanding of the differential signals regulating alphabeta/gammadelta T lineage choice. *Semin Immunol* 22: 237–246
- Ikawa T, Hirose S, Masuda K, Kakugawa K, Satoh R, Shibano-Satoh A, Kominami R, Katsura Y, Kawamoto H (2010) An essential developmental checkpoint for production of the T cell lineage. *Science* 329: 93–96

24. Li L, Leid M, Rothenberg EV (2010) An early T cell lineage commitment checkpoint dependent on the transcription factor Bcl11b. *Science* 329: 89–93
25. Taghon T, Rothenberg EV (2008) Molecular mechanisms that control mouse and human TCR- $\alpha$  and TCR- $\gamma$  T cell development. *Semin Immunopathol* 30: 383–398
26. Taghon T, Stolz F, De Smedt M, Cnockaert M, Verhasselt B, Plum J, Leclercq G (2002) HOX-A10 regulates hematopoietic lineage commitment: evidence for a monocyte-specific transcription factor. *Blood* 99: 1197–1204
27. Plum J, De Smedt M, Defresne MP, Leclercq G, Vandekerckhove B (1994) Human CD34<sup>+</sup> fetal liver stem cells differentiate to T cells in a mouse thymic microenvironment. *Blood* 84: 1587–1593
28. Van de Walle I, De Smet G, Gartner M, De Smedt M, Waegemans E, Vandekerckhove B, Leclercq G, Plum J, Aster JC, Bernstein ID, et al (2011) Jagged2 acts as a Delta-like Notch ligand during early hematopoietic cell fate decisions. *Blood* 117: 4449–4459
29. Coffey F, Lee SY, Buus TB, Lauritsen JP, Wong GW, Joachims ML, Thompson LF, Zuniga-Pflucker JC, Kappes DJ, Wiest DL (2014) The TCR ligand-inducible expression of CD73 marks  $\gamma$  T cell lineage commitment and a metastable intermediate in effector specification. *J Exp Med* 211: 329–343
30. Taghon T, Van de Walle I, De Smet G, De Smedt M, Leclercq G, Vandekerckhove B, Plum J (2009) Notch signaling is required for proliferation but not for differentiation at a well-defined beta-selection checkpoint during human T cell development. *Blood* 113: 3254–3263
31. Cante-Barrett K, Mendes RD, Li Y, Vroegindewij E, Pike-Overzet K, Wabeke T, Langerak AW, Pieters R, Staal FJ, Meijerink JP (2017) Loss of CD44(dim) expression from early progenitor cells marks T cell lineage commitment in the human thymus. *Front Immunol* 8: 32
32. Casero D, Sandoval S, Seet CS, Scholes J, Zhu Y, Ha VL, Luong A, Parekh C, Crooks GM (2015) Long non-coding RNA profiling of human lymphoid progenitor cells reveals transcriptional divergence of B cell and T cell lineages. *Nat Immunol* 16: 1282–1291
33. Dik WA, Pike-Overzet K, Weerkamp F, de Ridder D, de Haas EF, Baert MR, van der Spek P, Koster EE, Reinders MJ, van Dongen JJ, et al (2005) New insights on human T cell development by quantitative T cell receptor gene rearrangement studies and gene expression profiling. *J Exp Med* 201: 1715–1723
34. Sun Z, Unutmaz D, Zou YR, Sunshine MJ, Pierani A, Brenner-Morton S, Mebius RE, Littman DR (2000) Requirement for ROR $\gamma$  in thymocyte survival and lymphoid organ development. *Science* 288: 2369–2373
35. Kreslavsky T, Savage AK, Hobbs R, Gounari F, Bronson R, Pereira P, Pandolfi PP, Bendelac A, von Boehmer H (2009) TCR-inducible PLZF transcription factor required for innate phenotype of a subset of  $\gamma$  T cells with restricted TCR diversity. *Proc Natl Acad Sci USA* 106: 12453–12458
36. Mingueneau M, Kreslavsky T, Gray D, Heng T, Cruse R, Ericson J, Bendall S, Spitzer MH, Nolan GP, Kobayashi K, et al (2013) The transcriptional landscape of  $\alpha$  T cell differentiation. *Nat Immunol* 14: 619–632
37. Wang H, Zou J, Zhao B, Johannsen E, Ashworth T, Wong H, Pear WS, Schug J, Blacklow SC, Arnett KL, et al (2011) Genome-wide analysis reveals conserved and divergent features of Notch1/RBPJ binding in human and murine T-lymphoblastic leukemia cells. *Proc Natl Acad Sci USA* 108: 14908–14913
38. Wakabayashi Y, Watanabe H, Inoue J, Takeda N, Sakata J, Mishima Y, Hitomi J, Yamamoto T, Utsuyama M, Niwa O, et al (2003) Bcl11b is required for differentiation and survival of  $\alpha$  T lymphocytes. *Nat Immunol* 4: 533–539
39. Kueh HY, Yui MA, Ng KK, Pease SS, Zhang JA, Damle SS, Freedman G, Siu S, Bernstein ID, Elowitz MB, et al (2016) Asynchronous combinatorial action of four regulatory factors activates Bcl11b for T cell commitment. *Nat Immunol* 17: 956–965
40. Johnson JL, Georgakilas G, Petrovic J, Kurachi M, Cai S, Harly C, Pear WS, Bhandoola A, Wherry EJ, Vahedi G (2018) Lineage-determining transcription factor TCF-1 initiates the epigenetic identity of T cells. *Immunity* 48: 243–257.e10
41. Zhang JA, Mortazavi A, Williams BA, Wold BJ, Rothenberg EV (2012) Dynamic transformations of genome-wide epigenetic marking and transcriptional control establish T cell identity. *Cell* 149: 467–482
42. Germar K, Dose M, Konstantinou T, Zhang J, Wang H, Lobry C, Arnett KL, Blacklow SC, Aifantis I, Aster JC, et al (2011) T cell factor 1 is a gatekeeper for T cell specification in response to Notch signaling. *Proc Natl Acad Sci USA* 108: 20060–20065
43. Weber BN, Chi AW, Chavez A, Yashiro-Ohtani Y, Yang Q, Shestova O, Bhandoola A (2011) A critical role for TCF-1 in T-lineage specification and differentiation. *Nature* 476: 63–68
44. Mavrakis KJ, Van Der Meulen J, Wolfe AL, Liu X, Mets E, Taghon T, Khan AA, Setty M, Rondou P, Vandenberghe P, et al (2011) A cooperative microRNA-tumor suppressor gene network in acute T cell lymphoblastic leukemia (T-ALL). *Nat Genet* 43: 673–678
45. Seet CS, He C, Bethune MT, Li S, Chick B, Gschweng EH, Zhu Y, Kim K, Kohn DB, Baltimore D, et al (2017) Generation of mature T cells from human hematopoietic stem and progenitor cells in artificial thymic organoids. *Nat Methods* 14: 521–530
46. Ciofani M, Zuniga-Pflucker JC (2005) Notch promotes survival of pre-T cells at the beta-selection checkpoint by regulating cellular metabolism. *Nat Immunol* 6: 881–888
47. Ha VL, Luong A, Li F, Casero D, Malvar J, Kim YM, Bhatia R, Crooks GM, Parekh C (2017) The T-ALL related gene BCL11B regulates the initial stages of human T cell differentiation. *Leukemia* 31: 2503–2514
48. Di Santo JP (2010) Immunology. A guardian of T cell fate. *Science* 329: 44–45
49. Li P, Burke S, Wang J, Chen X, Ortiz M, Lee SC, Lu D, Campos L, Goulding D, Ng BL, et al (2010) Reprogramming of T cells to natural killer-like cells upon Bcl11b deletion. *Science* 329: 85–89
50. Isoda T, Moore AJ, He Z, Chandra V, Aida M, Denholtz M, Piet van Hamburg J, Fisch KM, Chang AN, Fahl SP, et al (2017) Non-coding transcription instructs chromatin folding and compartmentalization to dictate enhancer-promoter communication and T cell fate. *Cell* 171: 103–119.e18
51. Avram D, Califano D (2014) The multifaceted roles of Bcl11b in thymic and peripheral T cells: impact on immune diseases. *J Immunol* 193: 2059–2065
52. Rothenberg EV, Ungerback J, Champhekar A (2016) Forging T-lymphocyte identity: intersecting networks of transcriptional control. *Adv Immunol* 129: 109–174
53. Rothenberg EV, Kueh HY, Yui MA, Zhang JA (2016) Hematopoiesis and T cell specification as a model developmental system. *Immunol Rev* 271: 72–97
54. Weng AP, Millholland JM, Yashiro-Ohtani Y, Arcangeli ML, Lau A, Wai C, Del Bianco C, Rodriguez CG, Sai H, Tobias J, et al (2006) c-Myc is an important direct target of Notch1 in T cell acute lymphoblastic leukemia/lymphoma. *Genes Dev* 20: 2096–2109
55. O'Donnell KA, Wentzel EA, Zeller KI, Dang CV, Mendell JT (2005) c-Myc-regulated microRNAs modulate E2F1 expression. *Nature* 435: 839–843

56. Regelin M, Blume J, Pommerencke J, Vakilizadeh R, Witzlau K, Lyszkiewicz M, Zietara N, Saran N, Schambach A, Krueger A (2015) Responsiveness of developing T cells to IL-7 signals is sustained by miR-17 approximately 92. *J Immunol* 195: 4832–4840
57. Gonzalez-Garcia S, Garcia-Peydro M, Martin-Gayo E, Ballestar E, Esteller M, Bornstein R, de la Pompa JL, Ferrando AA, Toribio ML (2009) CSL-MAML-dependent Notch1 signaling controls T lineage-specific IL-7R {alpha} gene expression in early human thymopoiesis and leukemia. *J Exp Med* 206: 779–791
58. De Smedt M, Hoebeke I, Reynvoet K, Leclercq G, Plum J (2005) Different thresholds of Notch signaling bias human precursor cells toward B-, NK-, monocytic/dendritic-, or T cell lineage in thymus microenvironment. *Blood* 106: 3498–3506
59. Gutierrez A, Kentsis A, Sanda T, Holmfeldt L, Chen SC, Zhang J, Prottopov A, Chin L, Dahlberg SE, Neuberger DS, et al (2011) The BCL11B tumor suppressor is mutated across the major molecular subtypes of T cell acute lymphoblastic leukemia. *Blood* 118: 4169–4173
60. Fuziwara CS, Kimura ET (2015) Insights into regulation of the miR-17-92 cluster of miRNAs in cancer. *Front Med (Lausanne)* 2: 64
61. Lessel D, Gehbauer C, Bramswig NC, Schluth-Bolard C, Venkataramanappa S, van Gassen KLI, Hempel M, Haack TB, Baresic A, Genetti CA, et al (2018) BCL11B mutations in patients affected by a neurodevelopmental disorder with reduced type 2 innate lymphoid cells. *Brain* 141: 2299–2311
62. Punwani D, Zhang Y, Yu J, Cowan MJ, Rana S, Kwan A, Adhikari AN, Lizama CO, Mendelsohn BA, Fahl SP, et al (2016) Multisystem anomalies in severe combined immunodeficiency with mutant BCL11B. *N Engl J Med* 375: 2165–2176
63. Mets E, Van der Meulen J, Van Peer G, Boice M, Mestdagh P, Van de Walle I, Lammens T, Goossens S, De Moerloose B, Benoit Y, et al (2015) MicroRNA-193b-3p acts as a tumor suppressor by targeting the MYB oncogene in T cell acute lymphoblastic leukemia. *Leukemia* 29: 798–806
64. Mestdagh P, Van Vlierberghe P, De Weer A, Muth D, Westermann F, Speleman F, Vandesompele J (2009) A novel and universal method for microRNA RT-qPCR data normalization. *Genome Biol* 10: R64
65. Wu Y, Cain-Hom C, Choy L, Hagenbeek TJ, de Leon GP, Chen Y, Finkle D, Venook R, Wu X, Ridgway J, et al (2010) Therapeutic antibody targeting of individual Notch receptors. *Nature* 464: 1052–1057
66. Mancini SJ, Mantei N, Dumortier A, Suter U, MacDonald HR, Radtke F (2005) Jagged1-dependent Notch signaling is dispensable for hematopoietic stem cell self-renewal and differentiation. *Blood* 105: 2340–2342
67. Xu J, Krebs LT, Gridley T (2010) Generation of mice with a conditional null allele of the Jagged2 gene. *Genesis* 48: 390–393
68. Gordon J, Xiao S, Hughes B III, Su DM, Navarre SP, Condie BG, Manley NR (2007) Specific expression of lacZ and cre recombinase in fetal thymic epithelial cells by multiplex gene targeting at the Foxn1 locus. *BMC Dev Biol* 7: 69
69. Mullokandov G, Baccarini A, Ruzo A, Jayaprakash AD, Tung N, Israelow B, Evans MJ, Sachidanandam R, Brown BD (2012) High-throughput assessment of microRNA activity and function using microRNA sensor and decoy libraries. *Nat Methods* 9: 840–846